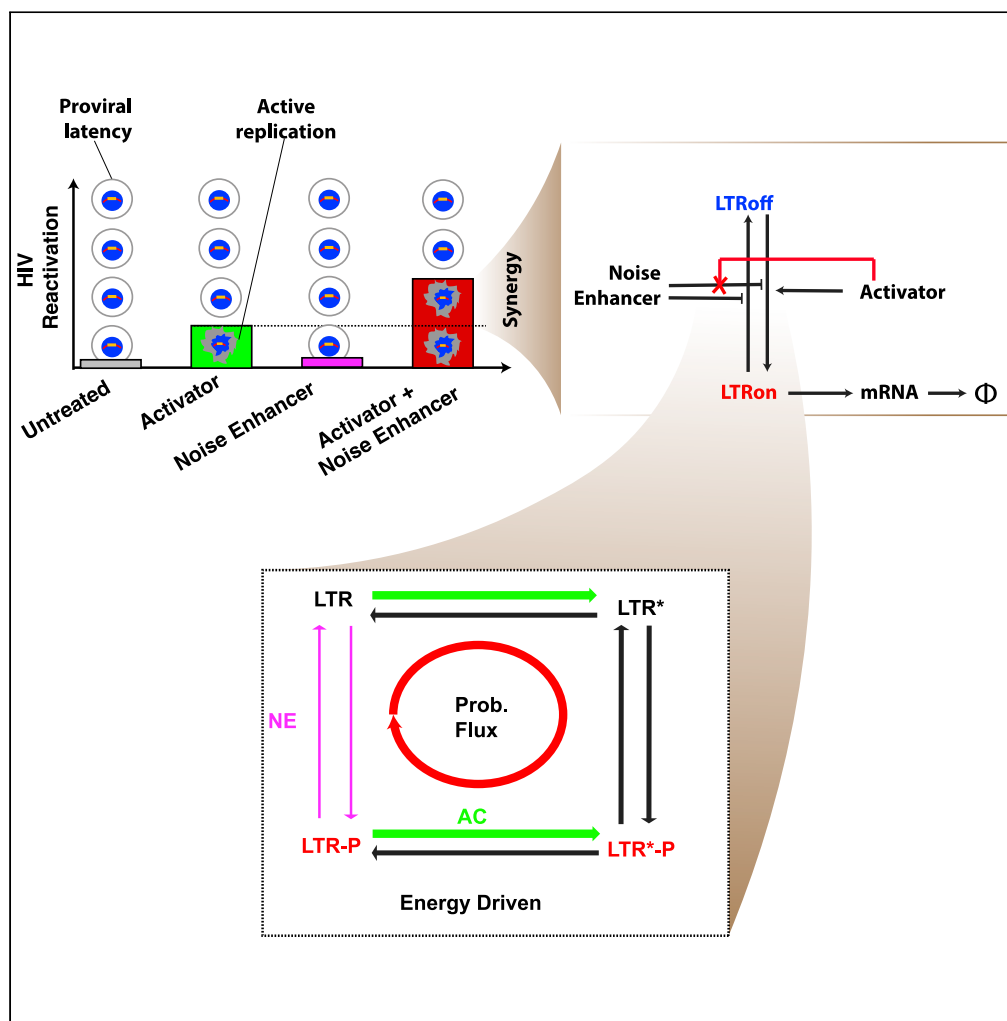## Article

The nonequilibrium mechanism of noise-enhanced drug synergy in HIV latency reactivation

Xiaolu Guo, Tao Tang, Minxuan Duan, Lei Zhang, Hao Ge

zhangl@math.pku.edu.cn (L.Z.)
haoge@pku.edu.cn (H.G.)

Highlights

The inhibition of Activator on Noise enhancer is necessary for their synergy in reactivating HIV

The drug synergy is a nonequilibrium phenomenon in the gene regulatory system

The magnitude and direction of energy input determine the drug synergy

This nonequilibrium mechanism is general without regarding molecular details

Article

The nonequilibrium mechanism of noise-enhanced drug synergy in HIV latency reactivation

Xiaolu Guo,[1] Tao Tang,[2] Minxuan Duan,[3] Lei Zhang,[4,5,*] and Hao Ge[4,6,7,*]

SUMMARY

Noise-modulating chemicals can synergize with transcriptional activators in reactivating latent HIV to eliminate latent HIV reservoirs. To understand the underlying biomolecular mechanism, we investigate a previous two-gene-state model and identify two necessary conditions for the synergy: an assumption of the inhibition effect of transcription activators on noise enhancers; and frequent transitions to the gene non-transcription-permissive state. We then develop a loop-four-gene-state model with Tat transcription/translation and find that drug synergy is mainly determined by the magnitude and direction of energy input into the genetic regulatory kinetics of the HIV promoter. The inhibition effect of transcription activators is actually a phenomenon of energy dissipation in the nonequilibrium gene transition system. Overall, the loop-four-state model demonstrates that energy dissipation plays a crucial role in HIV latency reactivation, which might be useful for improving drug effects and identifying other synergies on lentivirus latency reactivation.

INTRODUCTION

At the end of 2017, more than 36 million people were estimated to be infected with HIV (UNAIDS, 2018). After HIV infects CD4^{+} cells, it can replicate or enter proviral latency (Figure 1A). Latent HIV reservoirs are the main obstacle to achieving a clinical cure (Richman et al., 2009). Reactivating latent HIV, quickly followed by antiretroviral therapy (the "shock and kill" strategy), has become a promising way to cure HIV-infected patients (Deeks, 2012). Thus, understanding the HIV latency reactivation mechanism is vital and necessary for more effective drug target design using the "shock" strategy.

The main ingredients of the HIV regulatory loop are the long terminal repeat (LTR) and Tat transactivation on LTR. LTR is the promoter of the HIV genome and has a larger expression noise than promoters of human genes (Pai and Weinberger, 2017; Dar et al., 2012a). Nucleosomes associated with the LTR often block the full transcription by RNA polymerase (RNAP), resulting in a low basal expression rate. The rarely produced Tat protein complexes with CDK9 and CyclinT1 form a *positive transcriptional elongation factor b* (pTEFb). pTEFb can bind to the transactivation response element (TAR) of the initially transcribed part of the HIV mRNA and remodel downstream nucleosomes. This remodeling assists elongating the mRNA, thus forming positive feedback (Kao et al., 1987; Kaehlcke et al., 2003; Karn, 2000). In addition, a bimodal gene expression ("phenotypic bifurcation" (Weinberger et al., 2005)) pattern was found in the offspring of defective-HIV infected cells with an initially intermediate expression (Weinberger et al., 2005). However, it was reported that the cooperativity coefficient (Hill coefficient) of Tat was only one (Weinberger and Shenk, 2007), which means that the mean-field deterministic dynamics of HIV gene expression are monostable. This is distinct from the genetic toggle switch of the lambda phage regulatory loop with stronger feedback and bistable deterministic dynamics (Gardner et al., 2000), or an oscillatory network with negative feedback and a limit cycle (Elowitz and Leibler, 2000). The deterministic dynamics of the HIV regulatory network are insufficient to explain the observed bimodality, so a stochastic description may be required. Several stochastic models, such as two- or three-LTR-state models with or without positive feedback (Skupsky et al., 2010; Dar et al., 2014; Singh et al., 2010; Razooky et al., 2015; Chavali et al., 2015), have been proposed to study the dynamics of HIV gene expression. By combining the bimodality and noisiness of the HIV promoter gene expression, Weinberger et al. found that bimodality arises from a very slow rate of switching on LTR expression (Weinberger et al., 2005), resulting in much noisier dynamics than those observed for normal human promoters.

[1]School of Mathematical Sciences, Peking University, Beijing 100871, China

[2]School of Life Sciences, Peking University, Beijing 100871, China

[3]Yuanpei College, Peking University, Beijing 100871, China

[4]Beijing International Center for Mathematical Research, Peking University, Beijing 100871, China

[5]Center for Quantitative Biology, Peking University, Beijing 100871, China

[6]Biomedical Pioneering Innovation Center, Peking University, Beijing 100871, China

[7]Lead contact

*Correspondence:
zhangl@math.pku.edu.cn (L.Z.),
haoge@pku.edu.cn (H.G.)
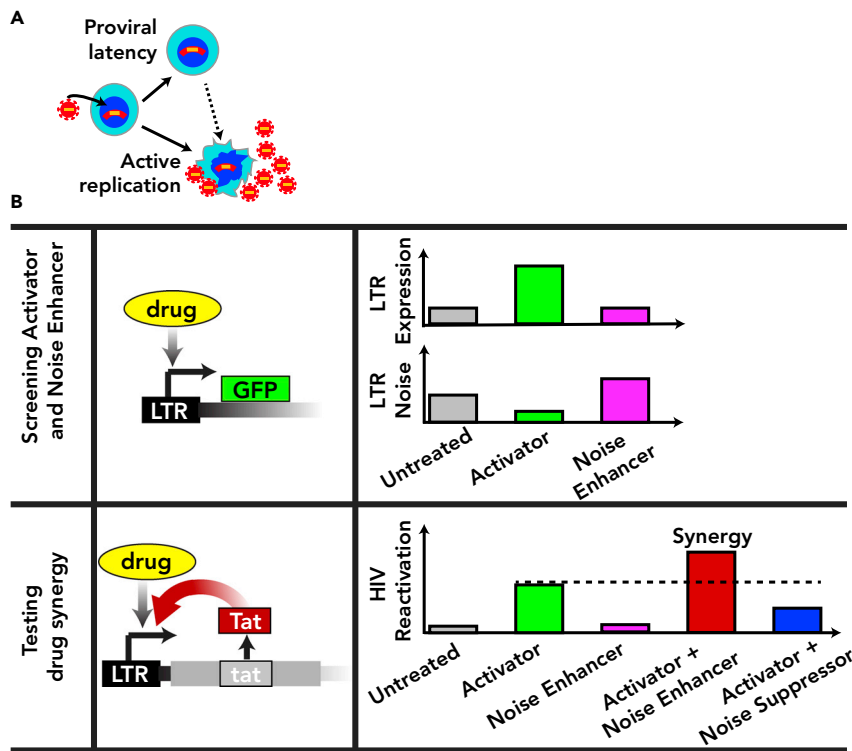https://doi.org/10.1016/j.isci.2022.104358

Figure 1. HIV-infected cell fates and biological function of biomolecules reactivating latent HIV

(A) Schematic of different fates of cells when infected by HIV: HIV active replication, HIV proviral latency, and HIV latency reactivation (adopted from Figure 1A of (Dar et al., 2014)).

(B) Diagram of screening Activators (AC) and Noise Enhancers (NE) (up) and testing synergy on the reactivation of latent HIV after adding AC or/and NE (down). In previous experiments, AC and NE were selected by detecting the mean and noise of LTR expression using cells infected by the LTR-GFP vector. The synergy between AC and NE on HIV reactivation was tested using cells infected by full-length HIV with Tat transactivation. Untreated cells (gray bar) represent a control group. In comparison to the control group, adding the Activator (green bar) increases LTR expression, while adding the Noise Enhancer (magenta bar) increases LTR noise. Adding AC and NE simultaneously (red bar) has a strong synergy on HIV reactivation (which increases the reactivation of latent HIV infected Cells compared to adding AC only). Adding AC and noise suppressors (NS, blue bar) has a depressing effect on HIV latency reactivation compared to adding AC only (Dar et al., 2014).

Recently, synergistic combinations of noise enhancers and activator drugs were reported not only to beat other reactivation cocktails in reactivating HIV latency but also to induce less cytotoxicity (Dar et al., 2014). Two specific types of drugs were involved in these synergistic combinations (Dar et al., 2014): Activators (AC), a small biological molecule that increases the average expression level of HIV proteins; and Noise Enhancers (NE), a different type of molecule that increases the noise of HIV protein expression but does not affect the average expression level. Although NE itself cannot reactivate latent HIV, it was shown to amplify AC-induced reactivation of HIV significantly (Dar et al., 2014). The synergy gained from adding NE and AC to latent HIV is shown in Figure 1B. However, the biomolecular mechanisms underlying the synergy between AC and NE have not been fully resolved. Functions of only a small fraction of AC and NE are partially known. For example, as activators, TNF and Prostratin can activate the transcriptional factor NF-κB, and therefore antagonize HIV latency (Williams et al., 2004; Duh et al., 1989; Osborn et al., 1989). Some of these Noise Enhancers, such as ethinyl estradiol, can influence HIV expression through another transcriptional factor SP1 or the structural state of chromatin (Asin et al., 2008; Katagiri et al., 2006). The detailed molecular mechanisms of most noise enhancers are still unclear, indicating the complicated regulation mechanism of HIV dynamics. However, the noise enhancers in (Dar et al., 2014) only influence the system by regulating the transcription machinery, because the post-transcription noise-enhancing molecules are filtered out by a two-reporter assay.

On the other hand, thermodynamic energy dissipation and timescale play a crucial role in gene expression progress. A general model, which considers the binding of multiple transcription factors (TF) under thermodynamic equilibrium in prokaryotic cells and the function that different pair TF interactions can achieve in gene expression of cells, has already been studied extensively (Buchler et al., 2003; Bintu et al., 2005).

However, in studies of eukaryotic transcriptional dynamics, a nonequilibrium mechanism was found necessary (Coulon et al., 2013), and many far-from-equilibrium models have been proposed (Scholes et al., 2017; Estrada et al., 2016; Ahsendorf et al., 2014; Li et al., 2018). In addition to biomolecule synthesis and cell motility, the regulatory function of a living cell, such as adaptation, and the precise control of oscillations were also found highly dissipative (Cao et al., 2015; Lan et al., 2012). Hence, we are very curious about whether certain energy input is necessary for noise-modulated drug synergy in HIV latency reactivation. In addition, in a self-positive feedback gene regulatory network, the timescale of DNA state transition, mRNA transcription, mRNA decay, protein translation, and protein decay will influence the cell fate landscape and phenotype transitions (Potoyan and Wolynes, 2017; Jia et al., 2018; Ge et al., 2015; Nie et al., 2020). Post-integration HIV gene expression is one example system of the TF regulatory mechanism of gene expression with self-positive feedback. Hence, we are also interested in how timescales of gene-state transition and protein dynamics influence drug synergy.

To explore the mechanism of noise-enhanced drug synergy in reactivating latent HIV, we investigate an established LTR-two-state model and then propose a loop-LTR-four-state model that explains the noise-enhanced drug synergy without direct interactions between AC and NE. Using these models, we then prove that, in the regulation of HIV promoter LTR, this synergy is controlled by the magnitude and direction of the system energy input. In essence, the LTR-four-state model is distinct from previous LTR state models, because the loop of the LTR four-state model allows for energy dissipation in the gene state transition network. Drug synergy can thus be significantly enhanced when we distribute the total energy input among two specific different reactions.

RESULTS

NE and AC can exhibit drug synergy on reactivating HIV latency in the LTR- -two-state model with significantly large k_{off}

We simulate the LTR-two-state model shown in Figure 2A using a Stochastic Simulation Algorithm (SSA) (Gillespie, 1977), calculating the reactivation of HIV latently infected T cells after adding NE and/or AC, with the appropriate assumptions on AC's and NE's functions (see STAR Methods section LTR-2 state model and simulation). Through simulation, we find that AC's inhibiting NE's function on k_{on} is necessary for synergy between AC and NE (Figures 2C–2D). When AC has no inhibiting effect on NE, which corresponds to $f_{inh} = 0$, there is no synergy between AC and NE in the whole reasonable parameter space (Figures 2C, 2B, black arrow). Only when AC inhibits NE's function of reducing k_{on} can there be synergy between AC and NE in reactivating latent HIV (Figures 2D, 2B, red arrow).

We also find that another necessary condition for NE to have significant synergy with AC is for k_{off} to be no less than 10^{-1} hour^{-1}. However, as other important results have shown in the previous literature, the bimodal distribution of phenotype bifurcation (Weinberger et al., 2005) and HIV latency establishment operating autonomously from the host cellular state (Razooky et al., 2015), are not sensitive to the increasing of k_{off} (Figures S1G–S1I). When k_{off} is less than 10^{-1}, there is no synergy between AC and NE in reactivating latent HIV (Figure 2E and S1E). However, if k_{off} is no less than 10^{-1}, then NE can have synergy with AC in reactivating latent HIV (Figures 2F–2G and S1F). Furthermore, the synergy between AC and NE will increase with the inhibiting effect quantity $f_{inh} > 0$ only when k_{off} is sufficiently large, such as when $k_{off} = 0.8 \geq 10^{-1}$ (Figure 2G, red line). There will be no synergy between AC and NE with the inhibiting effect quantity $f_{inh} > 0$ if $k_{off} < 10^{-1}$ (Figure 2E, red line). Actually, in a latent HIV system where the LTR transcription-permissive state should be unstable, k_{off} is more likely to be large owing to the weak expression integration site.

In summary, we find two necessary conditions of drug synergy from our simulation results: (i) AC inhibits NE's function of reducing k_{on}; (ii) there is a sufficiently large k_{off} (rate of LTR turning off or unbinding RNAP). However, the LTR-two-state model cannot uncover the mechanism of AC's inhibition on NE's function of reducing k_{on}, which is only an assumption made in (Dar et al., 2014). Furthermore, the very diverse NE selected from experiments also suggests that direct interaction between AC and the majority of NE is nearly impossible and a certain generic mechanism must be able to generate an equivalent effect.

No drug synergy can be produced under a detailed balance condition in the LTR- -four-state model coupling with Tat transactivation

The two LTR states are oversimplified so that the condition (i) AC inhibits NE's function of reducing k_{on} for the noise-enhanced drug synergy based on the two-state model is not very natural and also is not
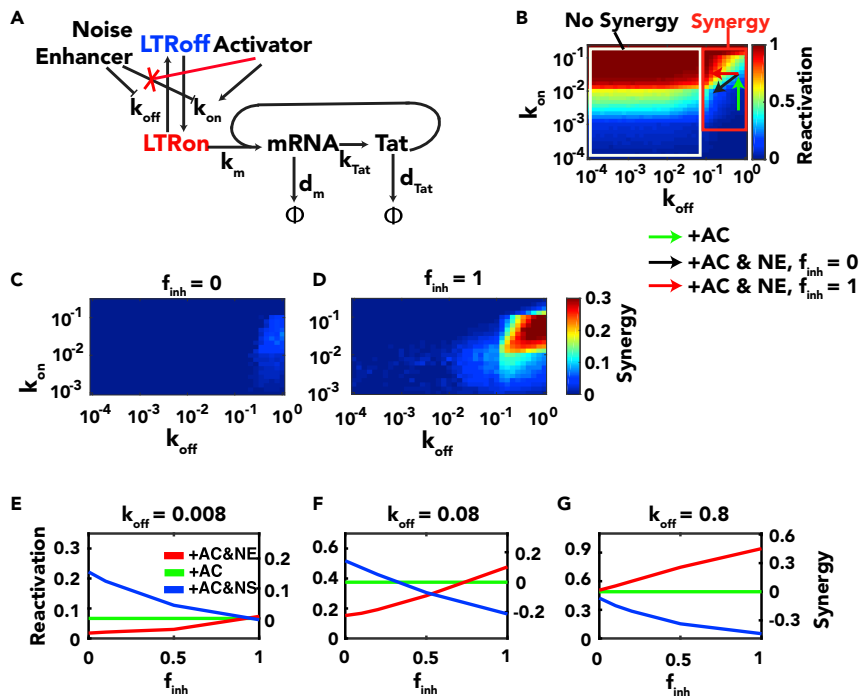
Figure 2. Two necessary conditions for drug synergy

(A) Modified from Figure 3A of (Razooky et al., 2015). The LTR-two-state model with Tat feedback is used to explain the effects of NE and AC molecules on HIV. LTR has two states, on and off, which convert to each other at the rate of k_{on} and k_{off}; the LTR-on state transcribes HIV mRNA at a rate of k_m, mRNA degrades at a rate of d_m or translates to protein at a rate of k_{Tat}, and Tat degrades at a rate of d_{Tat}. NE decreases k_{on} and k_{off} with their ratio fixed; AC molecules will increase k_{on}; AC inhibits NE's function on k_{on} when added together as assumed in (Dar et al., 2014). Tat transactivates LTR through enhancing the transcriptional rate $k_{trasact}$.

(B) The heatmap of reactivation across different values of LTR turning off at rate k_{off} and LTR turning on at rate k_{on}. The green arrow corresponds to adding AC. The red arrow corresponds to adding NE but only decreasing k_{off} without changing k_{on}, i.e., AC inhibits NE's function on k_{on}. The black arrow corresponds to adding NE, decreasing k_{off} and k_{on} with their ratio fixed, i.e., AC does not inhibit NE decreasing k_{on} (See Table S1 for parameter values.).

(C and D) The heatmap of synergy on reactivation without AC's inhibition on NE (f_{inh} = 0) and with AC's complete inhibition on NE (f_{inh} = 1), respectively, across different values of k_{off} and k_{on}, with AC added. The synergy is the reactivation plus NE and AC, subtracting the reactivation where only AC is added (See Table S1 for parameter values.).

(E–G) The plots of synergy on reactivation have different f_{inh} values for small k_{off}, intermediate k_{off}, and large k_{off}, respectively. The red lines indicate adding NE and AC simultaneously; the green lines indicate adding AC only; and the blue lines indicate adding NS and AC simultaneously (See Tables S1 and S2 for parameter values.).

convincing enough to explain why the drug synergy between activator and noise enhancer is almost universal as reported in (Dar et al., 2014). We implement a loop-LTR-four-state model coupled with a protein expression module (Figures 3A–3C and 4A) to understand the mechanism of drug synergy in reactivating HIV latency. The rationale for choosing the four-state model rather than another other form is just from biochemistry. The activators used in the experiments mostly act on transcriptional factors which will bind the DNA in order to facilitate the binding of RNAP, so the DNA needs to bind both RNAP and transcriptional factors. The four-gene-state model (Figures 3A–3C and 4A), in which each state represents a binding state of the promotor, is a widely-used description for modeling the promotor bounded both transcription factors (TF) and RNAP, just as in many previous studies on interactions between multiple TFs and RNAP in prokaryotic cells under thermodynamic equilibrium assumption (Buchler et al., 2003; Bintu et al., 2005), or the model for investigating the allostery of two proteins through their binding with DNA (Kim et al., 2013). Thus, it is natural to choose this well-established four-state model for our study of drug synergy.

More specifically, for example, the activator TNFα can stimulate NF-κB, which can remodel the chromatin structure to become more RNAP-accessible (Duh et al., 1989; Verdin et al., 1993), hence in this situation, in the LTR-four-state model (Figures 3A and 4A), LTR state is exactly the transcription-inactive state without
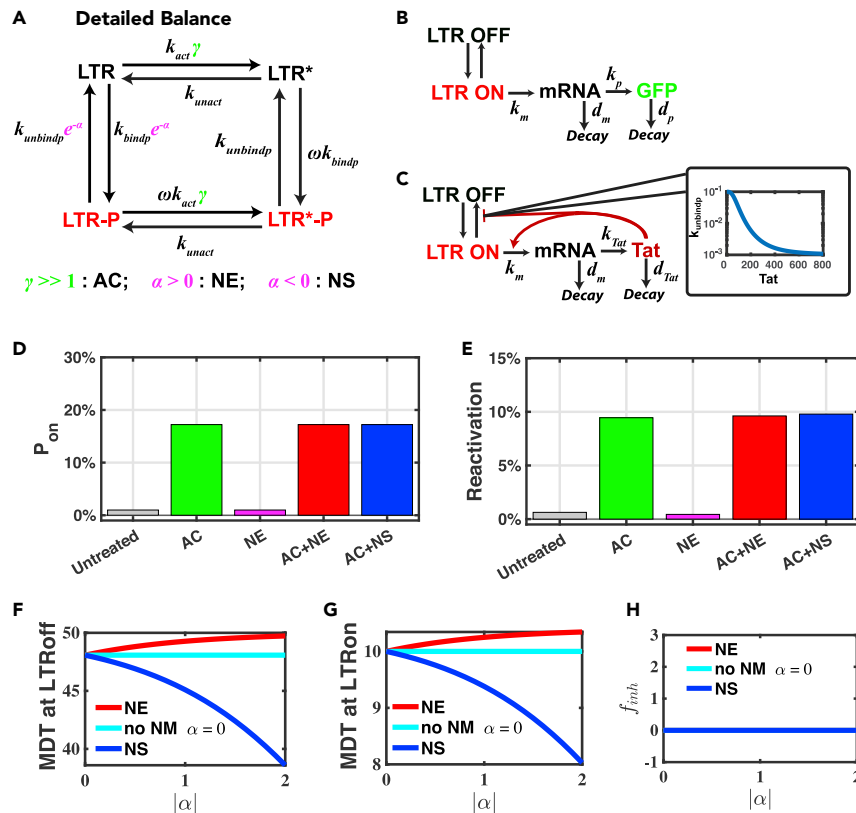
Figure 3. No synergy is predicted under the detailed balance condition

(A) Schematic of the LTR-four-state model with the Tat-feedback circuit. The LTR promoter is modeled for four states: a transcriptional silence state (LTR state), in which there are extremely slow binding RNAP polymerase or activation transcription factors such as NF-κB; an activated state (LTR*), such as LTR with an NF-κB bond; a transcription-permissive state (LTR-P); a transcription-permissive state with NF-κB bond (LTR*-P). Here, k_{act} is the rate for LTR binding NF-κB, while k_{unact} is the rate for LTR unbinding NF-κB. γ models AC as the rate for LTR binding NF-κB increases. $\gamma = 1$ for untreated HIV infected cells, and $\gamma \gg 1$ when adding AC. ω is the attraction coefficient between NF-κB and RNAP, $\omega = 10$ ($\omega > 1$ means NF-κB attracts RNAP); k_{bindp} is the rate at which RNAP binds to LTR; $k_{unbindp}$ is the rate at which RNAP unbinds from LTR; α is the noise attenuation factor ($\alpha > 0$ corresponds to the noise enhancer, and $\alpha < 0$ corresponds to noise suppressor). The parameters set here follow the detailed balance condition. The case of breaking the detailed balance can be seen in Figures 4 and S14.

(B) Schematic of the LTR-four-state model coupled with the transcription and translation module without feedback. LTR-on states (red, including LTR-P state and LTR*-P state) transcribes mRNA at rate k_m; mRNA decays at rate d_m or can be translated at rate k_p into GFP; GFP decays at rate d_p.

(C) Schematic of the LTR-four-state model coupled with the transcription and translation module with the Tat-transactivation circuit. LTR-on states (red, including LTR-P state and LTR*-P state) transcribes mRNA at rate k_m; mRNA decays at rate d_m or can be translated at rate k_{Tat} into Tat; Tat decays at rate d_{Tat}; Tat has positive feedback on k_m; Tat stabilizes the state of LTR-on state through negative feedback on $k_{unbindp}$.

(D and E) Probability of LTR-on states (LTR-P state andLTR*-P state), P_{on}, and reactivation ratio of Latent HIV, respectively, in the detailed-balanced LTR-four-state model. Y-axis is the P_{on} and the reactivation ratio value, respectively, and X-axis is the categories of different combinations of AC and NE/NS. Untreated cases (gray bars) correspond to $\gamma = 1, \alpha = 0$; adding only AC (green bars) corresponds to $\gamma \gg 1, \alpha = 0$; adding only NE (magenta bars) corresponds to $\gamma = 1, \alpha = 1$; adding NE and AC (red bars) corresponds to $\gamma \gg 1, \alpha = 1$; adding NS and AC (blue bars) corresponds to $\gamma \gg 1, \alpha = -1$. (E) We use the Stochastic Simulation Algorithm (SSA) to calculate the reactivation ratio of the LTR-four-state model coupled with Tat feedback. The reactivation ratio is the ratio of the reactivated HIV trajectory number at time 100h to all trajectory numbers, starting from the latency state (LTR = 1, all other species = 0, simulated 5000 cells).

(F and G) Mean duration time at LTR-off states and LTR-on states, respectively, under the detailed balance condition.

(H) f_{inh} is the degree of AC's inhibition upon the reduction of k_{on} induced by NE under the detailed balance condition. We first calculate the reciprocal of the mean duration time as the transition rate between LTR-on and LTR-off states, λ_{on} and λ_{off}, respectively. Then we calculate using the formula $f_{inh} = \frac{\ln(\lambda_{on,AC,NE}) - \ln(\lambda_{on,AC})}{\ln(\lambda_{off,AC}) - \ln(\lambda_{off,AC,NE})} + 1$ (see Equations 18 and 19 for more details). (F-H) The red lines correspond to adding AC and NE ($\alpha > 0$); the cyan lines correspond to adding AC only ($\alpha = 0$); the blue lines correspond to adding AC and NS ($\alpha < 0$) (See Tables S4 and S5 for parameter values.).
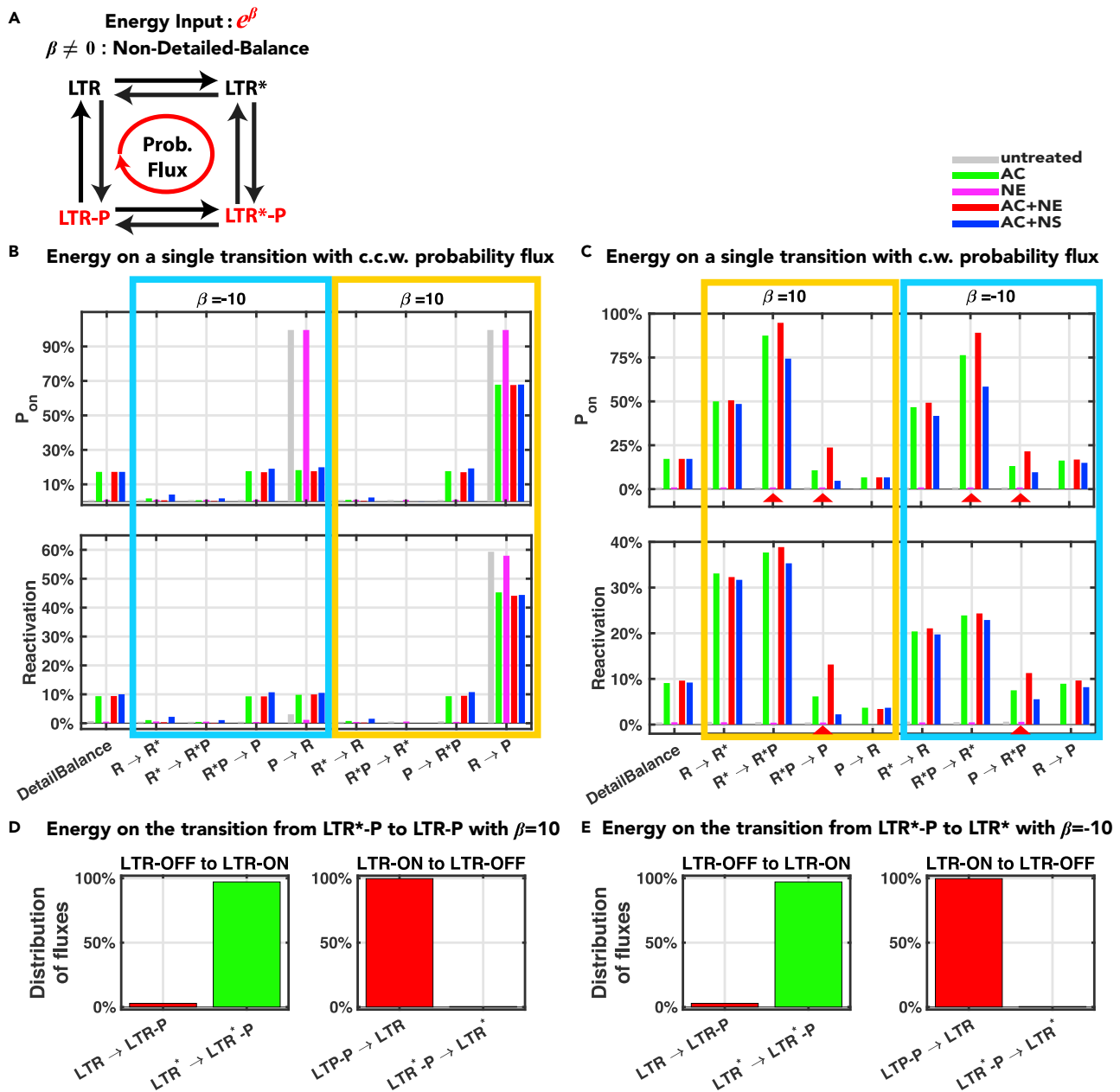
Figure 4. The LTR-four-state model with energy input on a single transition produces synergy between AC and NE if and only if the system has clockwise cyclic probability flux

(A) Schematic of the non-detailed-balanced LTR-four-state model. Energy input can influence any single transition rate of the detailed-balanced LTR-four-state model with the corresponding rate multiplying by e^{β} or $e^{-\beta}$. Such an energy input will cause clockwise (c.w.) cyclic probability flux or counter-clockwise (c.c.w.) cyclic probability flux.

(B and C) Probability of LTR-on states, P_{on} (up panels), and reactivation ratio of latent HIV (down panels) calculated from the non-detailed-balanced models with energy input on different single transitions causing a c.c.w. cyclic probability flux (B) or c.w. cyclic probability flux (C). R stands for LTR state; R* stands for LTR* state; P stands for LTR-P state; R*P stands for LTR*-P state. Each group of x-axis represents the non-detailed-balanced model with the corresponding transition rate multiplying by e^{β} ($\beta > 0$ for orange groups, $\beta < 0$ for blue groups). Red triangles indicate the significant synergy cases (See Figure S14 for precise values plotted) (See Figure S14 for model details. See Tables S4 and S5 for parameter values.).

(D and E) The distributions of fluxes for LTR turning on (left panels) and turning off (right panels) (See Figure S14 and STAR Methods section LTR-4 state model and simulation for model details. See Tables S4 and S5 for parameter values.).

RNAP binding, corresponding to a restricted and inaccessible chromatin configuration (Legube and Trouche, 2003); LTR* is the activated gene state without RNAP binding, corresponding to a more RNAP-accessible chromatin environment activated by host transcriptional factor, such as NF-κB; LTR-P and LTR*-P are the RNAP-binding states, respectively.

Similar to the well-analyzed assumptions of the AC's and NE's function from previous studies (Dar et al., 2014), AC is assumed to promote the transition of LTR or LTR-P to activated states, and NE is assumed to slow down the RNAP binding/unbinding activities between the inactive gene states (Figures 3A and 4A). Nevertheless, in this LTR-four-state model, there is no assumption of any direct interaction between AC and NE. We divide the LTR-four-state model into two categories. One is with the detailed balance condition (Figure 3A), and the other, which will be studied in the next subsection, is without the detailed balance condition (Figure 4A).

Under the detailed balance condition (Figure 3A), our LTR-four-state model with the transcription/translation module without Tat transactivation (Figure 3B; see STAR Methods section LTR-4-state model and simulation) illustrates that AC increases LTR mean expression level and that NE increases LTR expression noise (Figures S4C–S4D), which is consistent with the drug screening experimental results (Figure 1B) (Dar et al., 2014).

However, under the detailed balance condition, neither synergy between AC and NE nor depression of Noise Suppressor (NS) on AC, are possible in reactivating latent HIV (Figure 3). This contradicts the experimental data that shows that NE enhances AC's inducing latent HIV reactivation or that NSs reduce AC's reactivating of latent HIV (Figure 1B) (Dar et al., 2014). More specifically, under the detailed balance condition, P_{on} stays the same when both NE (or NS) and AC are added to the system ($\gamma \gg 1$, $\alpha = 1$ (or $\alpha = -1$)), compared to when only AC is added ($\gamma \gg 1$, $\alpha = 0$) (Figure 3D; see STAR Methods section LTR-4-state model and simulation for details). Thus, the detailed-balanced LTR-four-state model predicts no synergy between NE and AC and predicts that NS does not suppress the AC's function of increasing P_{on} (Figure 3D), contradicting the experimentally observed synergy between AC and NE (Figure 1B) (Dar et al., 2014). It is because under the detailed balance condition, the probability P_{on} of RNA polymerase binding to LTR (LTR-P and LTR*-P) (see STAR Methods section LTR-4-state model and simulation and section Mathematical analysis of LTR-4-state model) only depends on the equilibrium constants of each reaction, and NE or NS tunes the forward and backward rates simultaneously but keeps the equilibrium constant unvaried. This conclusion is not dependent on concrete models. It is a general physical and mathematical result. Hence it is not possible to build another even more complicated detailed-balanced model to overcome this obstacle.

We couple the detailed-balanced LTR-four-state model with Tat transactivation, and find there is still no synergy between NE and AC, as illustrated by the reactivation ratio of latent HIV (Figure 3E; see STAR Methods section Mathematical analysis of LTR-4-state model for details). Note that the reactivation ratio of HIV is calculated dynamically for a finite time, starting from the latent state, which is different from its steady-state probability P_{on}. However, both are closely related to each other, because they both indicate the degree of reactivation for latent HIV.

In addition, we calculate the mean duration time (MDT) of both the LTR-off states (LTR and LTR*) and the LTR-on states (LTR-P and LTR*-P) (see STAR Methods section Mathematical analysis of LTR-4-state model). The reciprocals of the MDTs calculated from the LTR-four-state model can be regarded as the effective transition rates in the reduced LTR-two-state model with only the LTR-off and LTR-on state. Next, we find out that AC can shorten the MDT at LTR-off states (Figures S4E and S4F), and that NE can lengthen the MDT at both LTR-on states and LTR-off states with their ratio fixed (Figures 3F–3G and S4G–S4H). These results are consistent with the assumptions of the LTR-two-state model in the previous section. However, in this detailed-balanced model, the effective inhibiting effect quantity f_{inh}, as defined by the effective transition rates, always vanishes (Figure 3H; see STAR Methods section Mathematical analysis of LTR-4-state model for the exact definition of f_{inh}). This confirms the LTR-two-state model predictions that no synergy between AC and NE in reactivating latent HIV should be observed when $f_{inh} = 0$.

Hence, for Noise Enhancers synergize with AC, the regulation of HIV gene expression must be a non-detailed-balanced process with energy dissipation.

The direction of the cycle flux caused by energy input in the non-detailed-balanced LTR- -four-state model determines the synergy

Inside a living cell, continuous energy consumption is necessary for executing different vital functions. We already know that systems with drug synergy must be energy dissipative, but how energy input, i.e., breaking the detailed balance, influences drug synergy remains poorly understood.

We mainly investigate how cycle flux direction and energy input distribution, as features of a nonequilibrium system, affect the synergy. Breaking the detailed balance is equivalent to having non-vanishing cycle fluxes. In our LTR-four-state model, the cycle fluxes can go either counter-clockwise or clockwise. Energy input can be distributed to one or more reactions. Here, we first consider the case of energy input for only one single reaction (Figure 4A; see STAR Methods section LTR-4-state model and simulation and Figure S14 for details). In the real biological system, the energy input can be realized through ATP hydrolysis or other reversible covalent modification (Berg et al., 2002).

We prove that the non-detailed-balanced LTR-four-state model can produce the drug synergy between NE and AC on P_{on}, if and only if the direction of cycle flux is clockwise. Mathematical analysis (see STAR Methods section Mathematical analysis of LTR-4-state model for details) and numerical simulations illustrate the same phenomenon. The model with counter-clockwise cycle flux predicts no synergy between NE and AC on P_{on} or HIV latency reactivation, and no reduction of P_{on} or latent HIV reactivation is observed when NS is added with AC (Figure 4B). On the other hand, with a clockwise cycle flux, the model predicts in all cases that NE can synergize with AC on P_{on}, and that 6 out of 8 cases NE synergize with AC on latent HIV reactivation (Figures 4C and S14). 4 out of 8 of the ways which break the detailed balance through a single reaction to produce a clockwise cyclic probability flux predicts that there is a significant synergy on P_{on} between NE and AC (Figure 4C up panel, Figure S14), and that NS reduces P_{on} with AC added. Two out of 8 of the ways i.e., increasing the transition rate from LTR*-P to LTR-P, or reducing the transition rate from LTR-P to LTR*-P, predicts that there is a significant synergy in the reactivation of latent HIV between NE and AC (Figure 4C down panel, Figure S14), and that NS reduces AC-induced HIV latency reactivation. The results of our model are consistent with the experimental fact that the majority of NE amplify AC reactivating latent HIV, while the majority of NSs suppress the reactivation of latent HIV with AC added. Thus, the non-detailed-balanced LTR-four-state model reveals that there is a general mechanism of the synergy between NE and AC on the reactivation of latent HIV, instead of a particular mechanism by a specific NE.

We also show that in the above cases of significant drug synergy between AC and NE, the clockwise cyclic probability flux always promotes LTR turn on mainly through the LTR*-to-LTR*-P pathway strengthened by AC and turn off through the LTR-P-to-LTR pathway weakened directly by NE (Figures 4D–4E). It explains why NE can further amplify the HIV latency reactivation induced by AC, as long as the energy input provides clockwise cyclic probability flux.

In addition, for the equilibrium system, the probability density function of the dwell time at LTR-off states is predicted to be monotonically decreasing and convex (Tu, 2008) (Figure S10, solid black lines). Monotonicity or convexity can be maintained for the nonequilibrium system with a low magnitude of energy input (a small disturbance to the equilibrium system; see Figure S10, dashed red line). However, as the magnitude of energy dissipation increases, the nonmonotonicity or concavity of the probability density function of dwell time could appear (Figures S10D and S10H, dotted red line, and solid red line).

The LTR-four-state model with distributed energy input may achieve much stronger synergy than that with energy input from a single reaction

One possible strategy by which strong synergy can be achieved is to drive the LTR promoter to turn on mostly through the LTR-to-LTR*-to-LTR*-P pathway, whose rate can be significantly increased by AC, and to turn off mostly through the LTR*P-to-LTR-P-to-LTR pathway (Figures 4D–4E), whose rate can be distinctly decreased by NE. This way, the promoter is more likely to transition to state LTR-P, rather than state LTR*, once it is at state LTR*-P. Here, we build an EITST (Energy Input on the Two Specific Transition rates) LTR-four-state model, in which part of the energy input reduces the transition rate from LTR*-P to LTR* (β_2) and the other part increases the transition rate from LTR*-P to LTR-P (β_1) (Figure 5A; see STAR Methods section LTR-4-state model and simulation for details), with the total energy fixed ($\beta_1 + \beta_2 = \beta$).
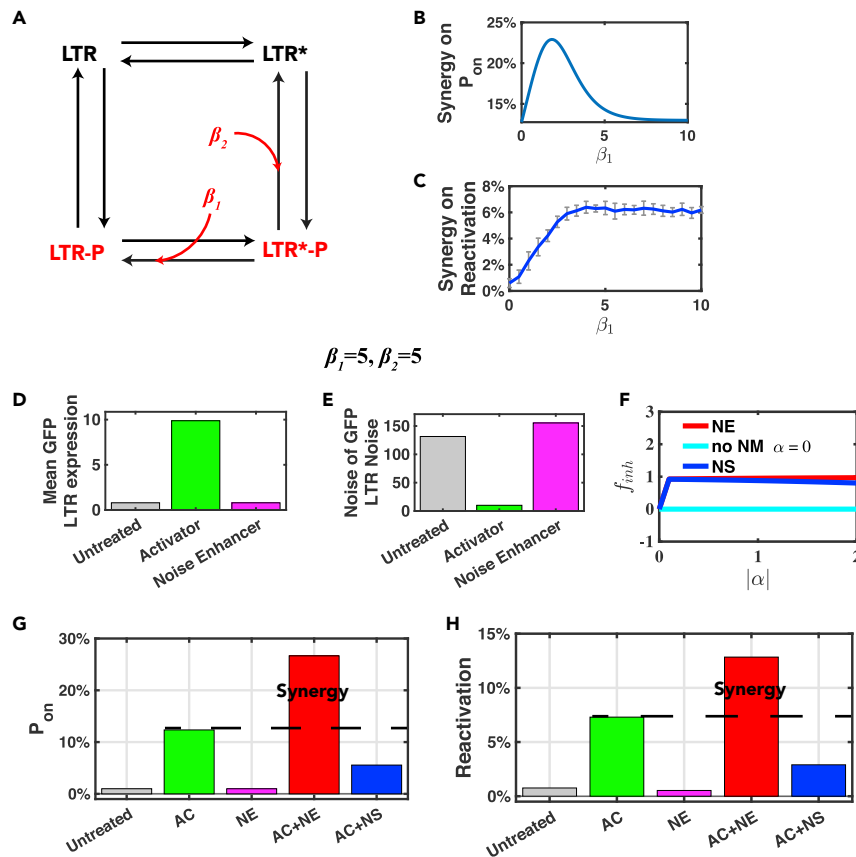
Figure 5. LTR-four-state model with distributed energy input exhibits strong synergy between AC and NE

(A) Schematic of the EITST model with distributed energy input ($\beta = \beta_1 + \beta_2 = 10$). The first part of the energy β_1 increases the LTR*-P-to-LTR-P transition rate by multiplying e^{β_1}; the other part of the energy β_2 reduces the LTR*-P-to-LTR* transition rate by multiplying $e^{-\beta_2}$.

(B and C) The synergy on P_{on} (B) and HIV latency reactivation (C) varies with energy distribution ($\beta_1 + \beta_2 = \beta = 10$). (C) Each point has an average of 250 simulation experimental data points, with 10,000 cells simulated for each experiment. Error bars show the standard deviation.

(D–J) $\beta_1 = \beta_2 = 5$.

(D and E) The mean and noise of GFP expression calculated from the EITST model without positive feedback.

(F) f_{inh} is the degree of AC's inhibition on the reduction of k_{on} induced by NE of the EITST model.

(G and H) Probability of LTR-on states (LTR-P state and LTR*-P state), P_{on}, and reactivation ratio of latent HIV, calculated from the EITST model (See Figure S14 for model details. See Tables S4 and S5 for parameter values.).

We find that there is an optimal energy input distribution ($\beta_1 = 1.8$, $\beta_2 = 8.2$) for the system to perform the strongest synergy between AC and NE on P_{on} (Figure 5B). The certain distributed energy input of $0 < \beta_1 < 10$ may achieve stronger synergy on P_{on} than that of a single reaction ($\beta_1 = 0$ or $\beta_1 = 10$). Drug synergy on HIV latency reactivation depends on an energy input distribution that will reach and then remain at the maximal level for $\beta_1 \gtrsim 4$ (Figure 5C). Without loss of generality, we set $\beta_1 = 5$ and $\beta_2 = 5$ for the EITST LTR-four-state model; all the following simulation results are based on these values.

In such a non-detailed-balanced model, simulation results of adding AC or NE alone with GFP present are consistent with the drug screening experimental data, that AC increases LTR mean expression level and NE increases LTR expression noise (Figures 5D–5E and 1B).

The synergy between a noise enhancer and an activator on both P_{on} (Figure 5G) and HIV latency reactivation (Figure 5H) have been observed to be much stronger than in the scenario where energy input is only from a single reaction. A noise enhancer can increase the HIV latency reactivation from approximately 7%, when an activator is already added, to 13%, when both are added (Figure 5H). These numbers are quite similar to the

best cases observed in experiments when Prostratin is used as the AC (experimental data from Figure 3A in (Dar et al., 2014)). In addition, such a mechanism of noise-enhanced drug synergy is very robust (Figure S12B) when we replace the first-order degradation of protein Tat with a more realistic stochastic process in which the protein Tat continuously accumulates during a cell cycle and only halve on cell division (Figure S12A) as suggested in previous studies (Beentjes et al., 2020; Perez-Carrasco et al., 2020; Sun et al., 2020; Padovan-Merhar et al., 2015). Furthermore, a noise suppressor reduces the AC-induced HIV latency reactivation from 7% to less than 1% (Figure 5H). This synergy between AC and NE on both P_{on} and HIV latency reactivation is found to be positively correlated with the magnitude $|\beta|$ of the total energy input, but reaches the maximum (for P_{on}) and saturation (for HIV latency reactivation) when $|\beta|$ is sufficiently large ($\beta > 5$) (Figures S6A–S6B). In addition, the synergy is found to be positively correlated with the noise of NE (Figure S6C); this is consistent with the experimental data (Figure 3B in (Dar et al., 2014)).

We also calculate the mean duration time (MDT) of the LTR-off and LTR-on states. In contrast to the detailed-balanced situation, NE can lengthen MDT at LTR-on states more significantly than at LTR-off states (Figures 5F and S7C–S7F). Furthermore, the effective inhibiting parameter $f_{inh} \approx 1 > 0$ (see STAR Methods section Mathematical analysis of LTR-4-state model for the exact definition of this effective parameter) means that AC does inhibit NE's function of reducing the transition rate from LTR-off states to LTR-on states (Figure 5F). These simulation results verify the conclusion we made in the LTR-two-state model: that NE can synergize with AC and NE in reactivating latent HIV only when $f_{inh} > 0$. Now we know that when AC inhibits NE's function of reducing effective k_{on}, this is achieved by the energy input that drives the clockwise cycle flux.

However, as in the LTR-two-state model, a noise enhancer can amplify an activator's reactivating of latent HIV only if $k_{unbindp}$ (equivalent to k_{off} in the LTR-two-state model) is greater than 10^{-2} (Figure S8A). To explain this necessary condition, we analyze the timescales of Tat transactivation dynamics and of LTR transitions. We find that it takes about $\tau_0 \approx 20$ hours on average of Tat transactivation for LTR to maintain an activated state for a long time (Figures S8B and S8C). Therefore, if $k_{unbindp}$ is very small compared to the timescale of $1/\tau_0$, the duration time of LTR-on state without NE present will be long enough for Tat transactivation to occur with a high probability; thus, further reducing $k_{unbindp}$ by NE will have little effect (Figure S8B). When $k_{unbindp}$ is not small compared to $1/\tau_0$, such a duration time is typically not long enough for Tat transactivation. In this case, lengthening the duration time of NE at the LTR-on state will provide Tat more time to reactivate latent HIV (Figure S8B), resulting in drug synergy with the activator.

Finally, to verify the model applicability, we use the same EITST model to explain other important previous experimental observations (Figures S3A–S3C), including Tat-transactivation-controlled HIV latency, which was established to operate autonomously from the host cellular state (Razooky et al., 2015), and bimodal distribution in the phenotype bifurcation of the Tat level (Weinberger et al., 2005) (see STAR Methods Tables S3–S4 for parameter values). Also, in our EITST model, the nonmonotonicity and concavity of the probability density function's dwell time are observed to have a large magnitude of energy dissipation (Figure S10F).

DISCUSSION

Long-lived latent HIV-1 is the main obstacle to a clinical cure (Richman et al., 2009). For noise-enhanced synergistic combinations of drugs that effectively reactivate HIV latency (Dar et al., 2014), we propose an LTR-four-state model with Tat transactivation (with only one cooperativity) to reveal the mechanism of this synergy, which is produced by the combination of AC and NE. Through analyzing and simulating this model, we find that the drug synergy on HIV latency reactivation depends on the distribution of energy input and the direction of the system's cycle flux.

As our model has illustrated, the synergy between AC and NE is universal, and our study supports the strategy of Dar et al. (2014) to discover novel drug combination for the treatment of virus infection, not only for HIV but also for the virus with a similar mechanism as HIV, such as the presence of latent state induced by the significant noise combined with a weak positive feedback mechanism. The AC and NE identified for other viruses can be different from those for HIV, but our model suggests that there should also be drug synergy between them.

Design principles for specific biological functions, such as reliable cell decisions (Brandman et al., 2005), adaptation (Ma et al., 2009), robust and tunable biological oscillation (Tsai et al., 2008), and the dual functions of adaptation and noise attenuation (Qiao et al., 2019), have been extensively explored. Some of these functions, such as biochemical oscillations and adaptation, were found to depend on energy dissipation (Cao et al., 2015; Lan et al., 2012). Here, we show that the drug synergy between NE and AC in reactivating HIV latency also depends on the direction in which chemical energy is dissipated during the HIV LTR-state transition. This nonequilibrium property could also be used as a potential target for lentivirus latency reversal in synergetic therapeutic interventions. The optimization principle of energy input distribution for the highest drug synergy might also apply to network designing.

Our LTR-four-state model is a minimal model in which the effects of AC and NE are modeled to account for drug synergy. What we discover, through this generic model, is the presence of a generic mechanism that is not restricted to specific molecules. Without specifying the exact pathway of NE in the LTR expression, we here adopted the validated assumption of NE as proposed in the study by Dar et al. (2014). NE that are filtered to have no influence on post-transcription rates are assumed to simultaneously reduce the transition rate between LTR on states and off states (Dar et al., 2014). Actually, the non-transcription-permissive activated state of LTR (LTR*) in our model can represent different biochemical states of LTR in the process of HIV gene expression, depending on different AC and NE. The general mechanism of noise-enhanced drug synergy we discovered is drawn from a rigorous mathematical proof (see STAR Methods section Mathematical analysis of LTR-4-state model) and is valid within a 0.1-fold to 10-fold change in the parameters (see Figure S13 for sensitivity analysis). In addition, this LTR-four-state model can be expanded into a more detailed LTR-six-state model, where the Tat positive feedback is modeled through Tat binding to LTR and forms two new states, LTR-P-Tat and LTR*-P-Tat, as shown in a previous study (Razooky et al., 2015). In the LTR-six-state model, the same synergy can be predicted (Figure S9 and STAR Methods section LTR-4-state model and simulation). Hence, the nonequilibrium mechanism of drug synergy we propose here is not dependent on a specific Tat positive feedback mechanism.

Most proteins are removed from the system primarily by dilution rather than active degradation mechanisms. We have shown that the mechanism for noise-enhanced drug synergy that we discovered is still valid if we replace the degradation process of protein with a noisier one owing to partitioning at cell division. In real cells, the situation should be more complicated, for instance, the transcription is coupled with the cell size. However, what we have illustrated is the same mechanism works for the two extreme circumstances: one is the relatively smooth noise with first-order degradation if the transcription and cell size are perfectly coupled with each other, and the other is the partition of protein at the cell division after accumulation during a whole-cell cycle without coupling to the cell size. Hence, we believe the same mechanism can be valid for the most general situations.

The nonequilibrium model proposed here is a minimal model providing an energy dissipation-based perspective to understand the general noise-enhanced drug synergy mechanism. In the LTR-two-state model, with or without Tat positive feedback, one necessary condition of the Noise-enhanced drug synergy in reactivating latent HIV is that AC blocks the NE's function of slowing down the rate of LTR when transitioning to a transcription-permissive state. However, this assumption cannot be justified or very well explained by previous two-state models. Improving on earlier studies, the loop LTR-four-state model, along with a specific directional probability flux (caused by the energy dissipation), shows that LTR primarily turns on through the pathway strengthened by AC and turns off primarily through the pathway weakened by NE, resulting in a synergy between AC and NE when the dwelling time of LTR-transcription-permissive states is lengthened, and making latent HIV reactivation more likely. In the models without such transition loops, the synergy cannot emerge without assuming an interaction between AC and NE. In addition, the nonequilibrium LTR-four-state model in this article estimates the influence of the energy dissipation ($\beta \neq 0$) on the gene expressing process, including the mean duration time and the gene expression pattern, while in the LTR-two-state model, the energy dissipation cannot be modeled at all. This is because, only in the loop multi-gene-state-transition model, the detailed balanced condition can be violated through energy dissipation, while for a multi-state model without loops (e.g. a two-gene-state model), the detailed balanced condition with a steady distribution is inherently satisfied.

Our model predicts how the magnitude of energy dissipation influences the gene expression process of LTR and drug synergy, which is not possible for the two-state model. Recently, Wang et al. (Wang et al.,

2016) experimentally tuned phosphorylation energy in living cells and studied how it influences cell-cycle dynamics. This kind of technique and experimental design could be applied to T-cells infected with LTR vectors in order to test the predicted relationship between drug synergy and energy dissipation in the LTR-four-state model.

Limitations of the study

In this study, we do not take the multi-loop model involving the process of more than one transcription factors (TFs) binding to the promoter LTR into consideration. The LTR has several TF binding sites, such as those for NFkB, AP1, and Sp1 (Karn and Stoltzfus, 2012; Gaynor, 1992). Some noise enhancers have an effect on the binding of different transcription factors (TFs) besides NFkB, such as Sp1 or AP1 (Dar et al., 2014; VanLint et al., 1997; Elkharroubi and Verdin, 1994; Katagiri et al., 2006). Modeling more than one TF binding process involves multiple loops, which is not considered in our research for simplicity. Actually, our model could easily be expanded to multi-loop model and then be utilized to investigate the drug synergy mechanism involving multiple TFs.

The LTR-four-state model is based on assumption that NE slow down the transition rates for RNAP binding/unbinding LTR. The Noise enhancer includes a wide range of pharmacological perturbations, such as antimitotic chemotherapy drugs or anti-histamine drugs (Dar et al., 2014). Although some of the Noise enhancer directly influence promoter accessibility, others perturb the transcription factor binding process indirectly. Other intricate molecular processes, such as Tat reactivation, could be involved. For example, the antihistamines (some specific NEs) can suppress CCL11 and CCL5, and CCL11 is a ligand for CCR2 (CCR2 binds Tat), CCR3, and CCR5 (Handen and Rosenberg, 1997). These detailed molecular processes are not included in the LTR-four-state model. It would be interesting to investigate the other processes for the potential drug synergy mechanism.

STAR★METHODS

Detailed methods are provided in the online version of this paper and include the following:

- KEY RESOURCES TABLE
- RESOURCE AVAILABILITY
  - Lead contact
  - Materials availability
  - Data and code availability
- METHOD DETAILS
  - LTR-2-state model and simulation
  - LTR-4-state model and simulation
- QUANTIFICATION AND STATISTICAL ANALYSIS
  - Mathematical analysis of LTR-4-state model

SUPPLEMENTAL INFORMATION

Supplemental information can be found online at https://doi.org/10.1016/j.isci.2022.104358.

AUTHOR CONTRIBUTIONS

H.G. and L.Z. conceived and supervised the project; X.G. performed the majority of data analysis and mathematical modeling with contributions by T.T.; X.G. performed the majority of analysis and computational simulations with contributions by M.D.; X.G., H.G., and L.Z. wrote the article.

DECLARATION OF INTERESTS

The authors declare no competing interests.

REFERENCES

Ahsendorf, T., Wong, F., Eils, R., and Gunawardena, J. (2014). A framework for modelling gene regulation which accommodates non-equilibrium mechanisms. BMC Biol. *12*, 102. https://doi.org/10.1186/s12915-014-0102-4.

Asin, S.N., Heimberg, A.M., Eszterhas, S.K., Rollenhagen, C., and Howell, A.L. (2008). Estradiol and progesterone regulate HIV type 1 replication in peripheral blood cells. AIDS Res. Hum. Retroviruses *24*, 701–716. https://doi.org/10.1089/aid.2007.0108.

Barboric, M., Nissen, R.M., Kanazawa, S., Jabrane-Ferrat, N., and Peterlin, B.M. (2001). NF-kappa B binds P-TEFb to stimulate transcriptional elongation by RNA polymerase II. Mol. Cell *8*, 327–337. https://doi.org/10.1016/s1097-2765(01)00314-8.

Beentjes, C.H.L., Perez-Carrasco, R., and Grima, R. (2020). Exact solution of stochastic gene expression models with bursting, cell cycle and replication dynamics. Phys. Rev. E *101*, 032403. https://doi.org/10.1103/physreve.101.032403.

Berg, J.M., Tymoczko, J.L., and Stryer, L. (2002). Covalent Modification is a Means of Regulating Enzyme Activity. Biochemistry, Fifth edition (W H Freeman).

Bintu, L., Buchler, N.E., Garcia, H.G., Gerland, U., Hwa, T., Kondev, J., and Phillips, R. (2005). Transcriptional regulation by the numbers: models. Curr. Opin. Genet. Dev. *15*, 116–124. https://doi.org/10.1016/j.gde.2005.02.007.

Brandman, O., Ferrell, J.E., Li, R., and Meyer, T. (2005). Interlinked fast and slow positive feedback loops drive reliable cell decisions. Science *310*, 496–498. https://doi.org/10.1126/science.1113834.

Buchler, N.E., Gerland, U., and Hwa, T. (2003). On schemes of combinatorial transcription logic. Proc. Natl. Acad. Sci. U S A *100*, 5136–5141. https://doi.org/10.1073/pnas.0930314100.

Cao, Y., Wang, H., Ouyang, Q., and Tu, Y. (2015). The free energy cost of accurate biochemical oscillations. Nat. Phys. *11*, 772–778. https://doi.org/10.1038/nphys3412.

Chavali, A.K., Wong, V.C., and Miller-Jensen, K. (2015). Distinct promoter activation mechanisms modulate noise-driven HIV gene expression. Sci. Rep. *5*, 17661. https://doi.org/10.1038/srep17661.

Coulon, A., Chow, C.C., Singer, R.H., and Larson, D.R. (2013). Eukaryotic transcriptional dynamics: from single molecules to cell populations. Nat. Rev. Genet. *14*, 572–584. https://doi.org/10.1038/nrg3484.

Cox, C.D., Mccollum, J.M., Allen, M.S., Dar, R.D., and Simpson, M.L. (2008). Using noise to probe and characterize gene circuits. Proc. Natl. Acad.

Sci. U S A *105*, 10809–10814. https://doi.org/10.1073/pnas.0804829105.

Dar, R.D., Hosmane, N.N., Arkin, M.R., Siliciano, R.F., and Weinberger, L.S. (2014). Screening for noise in gene expression identifies drug synergies. Science *344*, 1392–1396. https://doi.org/10.1126/science.1250220.

Dar, R.D., Karig, D.K., Cooke, J.F., Cox, C.D., and Simpson, M.L. (2010). Distribution and regulation of stochasticity and plasticity in Saccharomyces cerevisiae. Chaos *20*, 037106. https://doi.org/10.1063/1.3486800.

Dar, R.D., Razooky, B.S., Singh, A., Trimeloni, T.V., Mccollum, J.M., Cox, C.D., Simpson, M.L., and Weinberger, L.S. (2012a). Transcriptional burst frequency and burst size are equally modulated across the human genome. Proc. Natl. Acad. Sci. U S A *109*, 17454–17459. https://doi.org/10.1073/pnas.1213530109.

Dar, R.D., Razooky, B.S., Singh, A., Trimeloni, T.V., Mccollum, J.M., Cox, C.D., Simpson, M.L., and Weinberger, L.S. (2012b). Transcriptional burst frequency and burst size are equally modulated across the human genome. Proc. Natl. Acad. Sci. U S A *109*, 17454–17459. https://doi.org/10.1073/pnas.1213530109.

Deeks, S.G. (2012). HIV shock and kill. Nature *487*, 439–440. https://doi.org/10.1038/487439a.

Duh, E.J., Maury, W.J., Folks, T.M., Fauci, A.S., and Rabson, A.B. (1989). Tumor necrosis factor alpha activates human immunodeficiency virus type 1 through induction of nuclear factor binding to the NF-kappa B sites in the long terminal repeat. Proc. Natl. Acad. Sci. U S A *86*, 5974–5978. https://doi.org/10.1073/pnas.86.15.5974.

Elkharroubi, A., and Verdin, E. (1994). Protein-DNA interactions within dnase I-hypersensitive sites located downstream of the Hiv-1 promoter. J. Biol. Chem. *269*, 19916–19924. https://doi.org/10.1016/s0021-9258(17)32107-5.

Elowitz, M.B., and Leibler, S. (2000). A synthetic oscillatory network of transcriptional regulators. Nature *403*, 335–338. https://doi.org/10.1038/35002125.

Elowitz, M.B., Levine, A.J., Siggia, E.D., and Swain, P.S. (2002). Stochastic gene expression in a single cell. Science *297*, 1183–1186. https://doi.org/10.1126/science.1070919.

Estrada, J., Wong, F., Depace, A., and Gunawardena, J. (2016). Information integration and energy expenditure in gene regulation. Cell *166*, 234–244. https://doi.org/10.1016/j.cell.2016.06.012.

Feinberg, M.B., Baltimore, D., and Frankel, A.D. (1991). The role of tat in the human-immunodeficiency-virus life-cycle indicates a primary effect on transcriptional elongation. Proc.

Natl. Acad. Sci. U S A *88*, 4045–4049. https://doi.org/10.1073/pnas.88.9.4045.

Frankel, A.D. (1992). Activation of HIV transcription by tat. Curr. Opin. Genet. Dev. *2*, 293–298. https://doi.org/10.1016/0960-9822(92)90385-n.

Gardner, T.S., Cantor, C.R., and Collins, J.J. (2000). Construction of a genetic toggle switch in Escherichia coli. Nature *403*, 339–342. https://doi.org/10.1038/35002131.

Gaynor, R. (1992). Cellular transcription factors involved in the regulation of Hiv-1 gene-expression. AIDS *6*, 347–363. https://doi.org/10.1097/00002030-199204000-00001.

Ge, H., Qian, H., and Xie, X.S. (2015). Stochastic phenotype transition of a single cell in an intermediate region of gene state switching. Phys. Rev. Lett. *114*, 078101. https://doi.org/10.1103/physrevlett.114.078101.

Gillespie, D.T. (1977). Exact stochastic simulation of coupled chemical-reactions. J. Phys. Chem. *81*, 2340–2361. https://doi.org/10.1021/j100540a008.

Handen, J.S., and Rosenberg, H.F. (1997). Suppression of HIV-1 transcription by β-chemokines RANTES, MIP1-α, and MIP-1β is not mediated by the NFAT-1 enhancer element. FEBS Lett. *410*, 301–302. https://doi.org/10.1016/s0014-5793(97)00654-6.

Jia, C., Li, Y.H., and Qian, M.P. (2009). A general analysis of single IP3 receptors modulated by cytosolic Ca2+ and IP3. Optim. Syst. Biol. *11*, 89–101.

Jia, C., Liu, X.F., Qian, M.P., Jiang, D.Q., and Zhang, Y.P. (2012). Kinetic behavior of the general modifier mechanism of Botts and Morales with non-equilibrium binding. J. Theor. Biol. *296*, 13–20. https://doi.org/10.1016/j.jtbi.2011.11.006.

Jia, C., Qian, H., Chen, M., and Zhang, M.Q. (2018). Relaxation rates of gene expression kinetics reveal the feedback signs of autoregulatory gene networks. J. Chem. Phys. *148*, 095102. https://doi.org/10.1063/1.5009749.

Kaehlcke, K., Dorr, A., Hetzer-Egger, C., Kiermer, V., Henklein, P., Schnoelzer, M., Loret, E., Cole, P.A., Verdin, E., and Ott, M. (2003). Acetylation of Tat defines a cyclinT1-independent step in HIV transactivation. Mol. Cell *12*, 167–176. https://doi.org/10.1016/s1097-2765(03)00245-4.

Kaern, M., Elston, T.C., Blake, W.J., and Collins, J.J. (2005). Stochasticity in gene expression: from theories to phenotypes. Nat. Rev. Genet. *6*, 451–464. https://doi.org/10.1038/nrg1615.

Kao, S.Y., Calman, A.F., Luciw, P.A., and Peterlin, B.M. (1987). Anti-termination of transcription within the long terminal repeat of HIV-1 by tat gene product. Nature *330*, 489–493. https://doi.org/10.1038/330489a0.

Karn, J. (2000). Tat, a novel regulator of HIV transcription and latency. HIV Seq. Compend. 1990, 2–18.

Karn, J., and Stoltzfus, C.M. (2012). Transcriptional and posttranscriptional regulation of HIV-1 gene expression. Cold Spring Harb. Perspect. Med. 2, a006916. https://doi.org/10.1101/cshperspect.a006916.

Katagiri, D., Hayashi, H., Victoriano, A.F.B., Okamoto, T., and Onozaki, K. (2006). Estrogen stimulates transcription of human immunodeficiency virus type 1 (HIV-1). Int. Immunopharmacol. 6, 170–181. https://doi.org/10.1016/j.intimp.2005.07.017.

Kim, S., Brostromer, E., Xing, D., Jin, J.S., Chong, S.S., Ge, H., Wang, S.Y., Gu, C., Yang, L.J., Gao, Y.Q., et al. (2013). Probing allostery through DNA. Science 339, 816–819. https://doi.org/10.1126/science.1229223.

Lan, G., Sartori, P., Neumann, S., Sourjik, V., and Tu, Y.H. (2012). The energy-speed-accuracy trade-off in sensory adaptation. Nat. Phys. 8, 422–428. https://doi.org/10.1038/nphys2276.

Legube, G., and Trouche, D. (2003). Identification of a larger form of the histone acetyl transferase Tip60. Gene 310, 161–168. https://doi.org/10.1016/s0378-1119(03)00547-x.

Li, C.X., Cesbron, F., Oehler, M., Brunner, M., and Hofer, T. (2018). Frequency modulation of transcriptional bursting enables sensitive and rapid gene regulation. Cell Syst. 6, 409–423.e11. https://doi.org/10.1016/j.cels.2018.01.012.

Ma, W., Trusina, A., El-Samad, H., Lim, W.A., and Tang, C. (2009). Defining network topologies that can achieve biochemical adaptation. Cell 138, 760–773. https://doi.org/10.1016/j.cell.2009.06.013.

Nie, Q., Qiao, L., Qiu, Y., Zhang, L., and Zhao, W. (2020). Noise control and utility: from regulatory network to spatial patterning. Sci. China Math. 63, 425–440. https://doi.org/10.1007/s11425-019-1633-1.

Osborn, L., Kunkel, S., and Nabel, G.J. (1989). Tumor necrosis factor-alpha and interleukin-1 stimulate the human immunodeficiency virus enhancer by activation of the nuclear factor kappa-B. Proc. Natl. Acad. Sci. U S A 86, 2336–2340. https://doi.org/10.1073/pnas.86.7.2336.

Padovan-Merhar, O., Nair, G.P., Biaesch, A.G., Mayer, A., Scarfone, S., Foley, S.W., Wu, A.R., Churchman, L.S., Singh, A., and Raj, A. (2015). Single mammalian cells compensate for differences in cellular volume and DNA copy number through independent global transcriptional mechanisms. Mol. Cell 58, 339–352. https://doi.org/10.1016/j.molcel.2015.03.005.

Pai, A., and Weinberger, L.S. (2017). Fate-regulating circuits in viruses: from discovery to new therapy targets. Annu. Rev. Virol. 4, 469–490. https://doi.org/10.1146/annurev-virology-110615-035606.

Perez-Carrasco, R., Beentjes, C., and Grima, R. (2020). Effects of cell cycle variability on lineage and population measurements of messenger RNA abundance. J. R. Soc. Interface 17, 20200360. https://doi.org/10.1098/rsif.2020.0360.

Potoyan, D.A., and Wolynes, P.G. (2017). Stochastic dynamics of genetic broadcasting networks. Phys. Rev. E 96, 052305. https://doi.org/10.1103/physreve.96.052305.

Qiao, L.X., Zhao, W., Tang, C., Nie, Q., and Zhang, L. (2019). Network topologies that can achieve dual function of adaptation and noise attenuation. Cell Syst. 9, 271–285.e7. https://doi.org/10.1016/j.cels.2019.08.006.

Razooky, B.S., Pai, A., Aull, K., Rouzine, I.M., and Weinberger, L.S. (2015). A hardwired HIV latency program. Cell 160, 990–1001. https://doi.org/10.1016/j.cell.2015.02.009.

Richman, D.D., Margolis, D.M., Delaney, M., Greene, W.C., Hazuda, D., and Pomerantz, R.J. (2009). The challenge of finding a cure for HIV infection. Science 323, 1304–1307. https://doi.org/10.1126/science.1165706.

Scholes, C., Depace, A.H., and Sanchez, A. (2017). Combinatorial gene regulation through kinetic control of the transcription cycle. Cell Syst. 4, 97–108.e9. https://doi.org/10.1016/j.cels.2016.11.012.

Singh, A., Razooky, B., Cox, C.D., Simpson, M.L., and Weinberger, L.S. (2010). Transcriptional bursting from the HIV-1 promoter is a significant source of stochastic noise in HIV-1 gene expression. Biophys. J. 98, L32–L34. https://doi.org/10.1016/j.bpj.2010.03.001.

Skupsky, R., Burnett, J.C., Foley, J.E., Schaffer, D.V., and Arkin, A.P. (2010). HIV promoter integration site primarily modulates transcriptional burst size rather than frequency. PLoS Comput. Biol. 6, e1000952. https://doi.org/10.1371/journal.pcbi.1000952.

Sun, X.M., Bowman, A., Priestman, M., Bertaux, F., Martinez-Segura, A., Tang, W.H., Whilding, C., Dormann, D., Shahrezaei, V., and Marguerat, S. (2020). Size-dependent increase in RNA polymerase II initiation rates mediates gene expression scaling with cell size. Curr. Biol. 30, 1217–1230.e7. https://doi.org/10.1016/j.cub.2020.01.053.

Tsai, T.Y.C., Choi, Y.S., Ma, W.Z., Pomerening, J.R., Tang, C., and Ferrell, J.E. (2008). Robust, tunable biological oscillations from interlinked positive and negative feedback loops. Science 321, 126–129. https://doi.org/10.1126/science.1156951.

Tu, Y. (2008). The nonequilibrium mechanism for ultrasensitivity in a biological switch: sensing by Maxwell's demons. Proc. Natl. Acad. Sci. U S A 105, 11737–11741. https://doi.org/10.1073/pnas.0804641105.

UNAIDS (2018). UNAIDS data 2018. http://www.unaids.org/sites/default/files/media_asset/unaids-data-2018_en.pdf.

VanLint, C., Amella, C.A., Emiliani, S., John, M., Jie, T., and Verdin, E. (1997). Transcription factor binding sites downstream of the human immunodeficiency virus type 1 transcription start site are important for virus infectivity. J. Virol. 71, 6113–6127. https://doi.org/10.1128/jvi.71.8.6113-6127.1997.

Verdin, E., Paras, P., Jr., and Van Lint, C. (1993). Chromatin disruption in the promoter of human immunodeficiency virus type 1 during transcriptional activation. EMBO J. 12, 3249–3259. https://doi.org/10.1002/j.1460-2075.1993.tb05994.x.

Wang, T., Zhao, J., Ouyang, Q., Qian, H., Fu, Y.V., and Li, F. (2016). Phosphorylation energy and nonlinear kinetics as key determinants for G2/M transition in fission yeast cell cycle. Preprint at arXiv. https://doi.org/10.48550/arXiv.1610.09637.

Weinberger, L.S., Burnett, J.C., Toettcher, J.E., Arkin, A.P., and Schaffer, D.V. (2005). Stochastic gene expression in a lentiviral positive-feedback loop: HIV-1 Tat fluctuations drive phenotypic diversity. Cell 122, 169–182. https://doi.org/10.1016/j.cell.2005.06.006.

Weinberger, L.S., Dar, R.D., and Simpson, M.L. (2008). Transient-mediated fate determination in a transcriptional circuit of HIV. Nat. Genet. 40, 466–470. https://doi.org/10.1038/ng.116.

Weinberger, L.S., and Shenk, T. (2007). An HIV feedback resistor: auto-regulatory circuit deactivator and noise buffer. PLoS Biol. 5, e9. https://doi.org/10.1371/journal.pbio.0050009.

Williams, S.A., Chen, L.F., Kwon, H., Fenard, D., Bisgrove, D., Verdin, E., and Greene, W.C. (2004). Prostratin antagonizes HIV latency by activating NF-kappa B. J. Biol. Chem. 279, 42008–42017. https://doi.org/10.1074/jbc.m402124200.

Zhao, W., Qiao, L.X., Yan, S.Y., Nie, Q., and Zhang, L. (2021). Mathematical modeling of histone modifications reveals the formation mechanism and function of bivalent chromatin. iScience 24, 102732. https://doi.org/10.1016/j.isci.2021.102732.

STAR★METHODS

KEY RESOURCES TABLE

REAGENT or RESOURCE	SOURCE	IDENTIFIER
Software and algorithms		
MATLAB code for simulating LTR-two-state model and LTR-four-state models	This paper	https://github.com/Xiaolu-Guo/Noise-Enhanced-Drug-Synergy-in-HIV-Latency-Reactivation
MATLAB R2020a	MathWorks	https://www.mathworks.com/

RESOURCE AVAILABILITY

Lead contact

Further information can be provided by the Lead Contact, Hao Ge (haoge@pku.edu.cn).

Materials availability

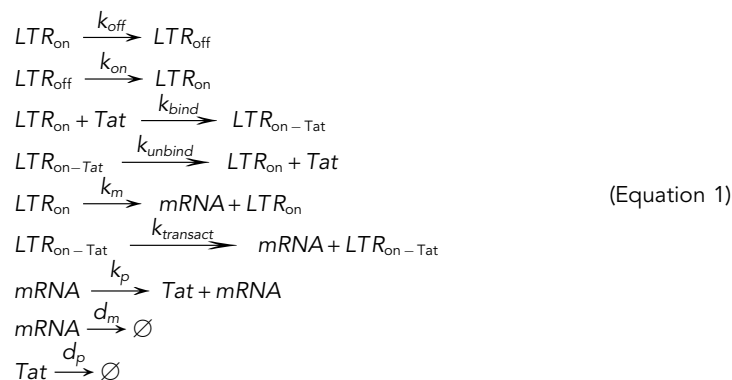This study did not generate new unique reagents.

Data and code availability

- All relevant data are within the paper and its supplemental information.

- The code is accessible here: https://github.com/Xiaolu-Guo/Noise-Enhanced-Drug-Synergy-in-HIV-Latency-Reactivation. Simulations in this paper are performed in software MATLAB (https://www.mathworks.com/).

- Any additional information required to reanalyze the data reported in this paper is available from the Lead contact upon request.

METHOD DETAILS

LTR-2-state model and simulation

LTR-2-state model

To investigate the synergy between AC and NE, we employed a well-established LTR-2-state model with Tat positive feedback from previous study (Figure 2A) (Dar et al., 2014; Razooky et al., 2015):

$$
\begin{aligned}
LTR_{on} &\xrightarrow{k_{off}} LTR_{off} \\
LTR_{off} &\xrightarrow{k_{on}} LTR_{on} \\
LTR_{on} + Tat &\xrightarrow{k_{bind}} LTR_{on-Tat} \\
LTR_{on-Tat} &\xrightarrow{k_{unbind}} LTR_{on} + Tat \\
LTR_{on} &\xrightarrow{k_m} mRNA + LTR_{on} \\
LTR_{on-Tat} &\xrightarrow{k_{transact}} mRNA + LTR_{on-Tat} \\
mRNA &\xrightarrow{k_p} Tat + mRNA \\
mRNA &\xrightarrow{d_m} \varnothing \\
Tat &\xrightarrow{d_p} \varnothing
\end{aligned}
\qquad \text{(Equation 1)}
$$

In this model, the promoter LTR can toggle between active and inactive states with transition rates k_{off} and k_{on}. Tat can bind/unbind to LTR (TAR) with rate k_{bind} and k_{unbind}, then transactivate LTR-on state once bound to TAR with a higher transcription rate $k_{transact}$ than the transcription rate k_m at LTR-on state due to Tat's enhancing LTR transcriptional elongation. mRNA can translate into protein at rate k_p. Also, mRNA and Tat will degrade at rate d_m and d_p respectively.

The functions of AC and NE in the LTR-2-state model

The values of parameters (k_{on}, k_{off}, $k_{transact}$) are the same as those in (Razooky et al., 2015), which is quantified by single-cell analysis (Dar et al., 2012b; Singh et al., 2010; Weinberger et al., 2008). In eukaryotic cells, one of the major sources of gene expression noise is the burst transcription arising from the stochastic transition between active and inactive promoter states that correspond to closed or open chromatin states (Kaern et al., 2005). Activators (AC) (e.g. Tumor Necrosis Factor (TNF)) can assist in the initiation of the transcript and then enhance the transcription frequency (Singh et al., 2010; Dar et al., 2012b). The burst frequency is determined by k_{on} in the LTR-two-state model. Thus, as dealt with in a previous study (Dar et al., 2014), AC is assumed to increase the parameter k_{on}, where the changing ratio modeled by r_{AC}. On the other hand, Dar et al. (2014) developed the two-reporter method (Elowitz et al., 2002; Cox et al., 2008; Dar et al., 2010) to filter noise enhancers not influenced by post transcription, and applied noise analysis in the HIV system (Singh et al., 2010; Dar et al., 2012b), combined with experimental tests. This filtering process suggests that the effects of NE reduce k_{on} and k_{off} by the same ratio, enhancing the noise without changing the average expression of HIV. We here adopt the sound assumption that NE slow down the switching rates between the two LTR states (Dar et al., 2014), where the changing ratio is represented by r_{NE}.

For clarity, we defined the rate variables as following:

k_{on} (k_{off}): the LTR turning on(off) rate in untreated HIV/LTR-GFP infected cells.

$k_{on,AC}$ ($k_{off,AC}$): the LTR turning on(off) rate with only Activator added to HIV/LTR-GFP infected cells.

$k_{on,NE}$ ($k_{off,NE}$): the LTR turning on(off) rate with only Noise Enhancer added to HIV/LTR-GFP infected cells.

$k_{on,AC,NE}$ ($k_{off,AC,NE}$): the LTR turning on(off) rate with both Activator and Noise Enhancer added to HIV/LTR-GFP infected cells.

$k_{on,NS}$, $k_{off,NS}$, $k_{on,AC,NS}$ and $k_{off,AC,NS}$ are defined in the same way.

In this LTR-2-state model, the functions of AC and NE are assumed as following (Dar et al., 2014): adding AC increases k_{on} to $k_{on}r_{AC}$, while adding NE reduces k_{on} and k_{off} to $k_{on}r_{NE}$ and $k_{off}r_{NE}$ ($r_{NE} < 1$), respectively, with their ratio fixed. From these assumptions, we have:

$$\begin{cases} k_{on,AC} = k_{on}r_{AC} \\ k_{off,AC} = k_{off} \end{cases}$$

and

$$\begin{cases} k_{on,NE} = k_{on}r_{NE} \\ k_{off,NE} = k_{off}r_{NE} \end{cases}$$

The values of $k_{on,AC,NE}$ and $k_{off,AC,NE}$ will be discussed in the next section.

f_{inh}, the degree of AC's inhibition upon the reduction of k_{on} induced by NE

It is worth noting that Dar et al. mentioned, "Enhanced activation requires and assumes that any changes in k_{on} by the noise enhancer are overly-compensated by the activator" (4). In order to investigate whether this inhibition effect from the activator on the noise enhancer's function of changing k_{on} is necessary for drug synergy, we use the parameter f_{inh} to quantify the degree of AC's inhibition upon the NE-induced reduction of k_{on}, as described following.

If the functions of AC and NE are working separately and independently, then

$$\begin{cases} k_{on,AC,NE} = k_{on}r_{AC}\gamma_{NE} \\ k_{off,AC,NE} = k_{off}r_{NE} \end{cases}$$

However, there might be some interaction between AC and NE's function. For AC and NE to has synergy on HIV latency reactivation, AC might inhibit NE's function on k_{on}. We quantified the inhibition of AC on NE's function on k_{on} as:

$$f_{inh} = 1 - \log_{r_{NE}}\left(\frac{k_{on,AC,NE}}{k_{on}r_{AC}}\right) = \frac{\ln(k_{on,AC,NE}) - \ln(k_{on,AC})}{\ln(k_{off,AC}) - \ln(k_{off,AC,NE})} + 1 \qquad \text{(Equation 2)}$$

Then we have:

$$\begin{cases} k_{on,AC,NE} = k_{on} r_{AC} r_{NE}^{1-f_{inh}} \\ k_{off,AC,NE} = k_{off} r_{NE} \end{cases}$$
$$f_{inh} \in [0,1]$$

$f_{inh} = 0$ represents AC does not inhibit NE's function of reducing k_{on} (Figure S1C, left panel), and $f_{inh} > 0$ means that AC does inhibit NE's function of reducing k_{on}. Particularly, $f_{inh} = 1$ means that NE's function of reducing k_{on} is completely inhibited by AC (Figure S1C, right panel).

Simulation of reactivation ratio

The stochastic LTR-2-state model coupled with Tat positive feedback (Equation 1) was simulated using the Stochastic Simulation Algorithm (SSA) (Gillespie, 1977).

Reactivation Ratio is the ratio of trajectory numbers with activated HIV (#Tat >75) up to 100 h and the total number of trajectories starting from the latency state ($LTR_{off} = 1$, copy numbers of all other species = 0, simulated 5000~10000 cells) at time 0h. These simulations were implemented via MATLAB™ with the parameters shown in Tables S1 and S2.

The synergy between AC and NE

From the experiments, the drug synergy is that NE can significantly amplify the reactivation of latent HIV caused by AC, while NE itself cannot reactivate latent HIV, i.e. 1 + 1>2 (Figure 1B) (Dar et al., 2014). Mathematically, we define the synergy on reactivating latent HIV as:
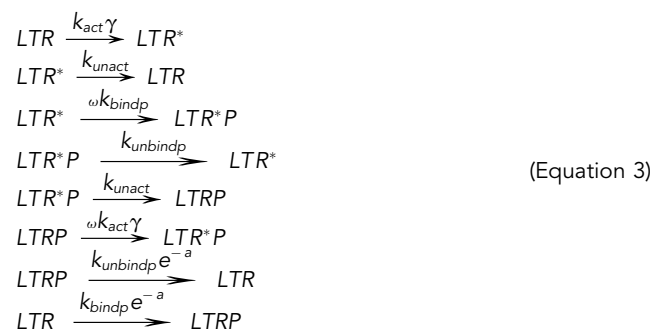
$$\text{Synergy} = R_{AC,NE} - R_{AC}$$

$R_{AC,NE}$ is the reactivation ratio of the latent HIV under parameter $k_{on,AC,NE}$ and $k_{off,AC,NE}$, corresponding to adding AC and NE together; R_{AC} is the reactivation ratio of the latent HIV under parameter $k_{on,AC}$ and $k_{off,AC}$, corresponding to adding only AC. The calculation of reactivation ratio has been explained in the last section.

LTR-4-state model and simulation

Detailed balance LTR-4-state model

We built an LTR-4-state model under detailed balance (Figure 3A):

$$\begin{aligned} LTR &\xrightarrow{k_{act}\gamma} LTR^* \\ LTR^* &\xrightarrow{k_{unact}} LTR \\ LTR^* &\xrightarrow{\omega k_{bindp}} LTR^*P \\ LTR^*P &\xrightarrow{k_{unbindp}} LTR^* \\ LTR^*P &\xrightarrow{k_{unact}} LTRP \\ LTRP &\xrightarrow{\omega k_{act}\gamma} LTR^*P \\ LTRP &\xrightarrow{k_{unbindp}e^{-a}} LTR \\ LTR &\xrightarrow{k_{bindp}e^{-a}} LTRP \end{aligned} \qquad \text{(Equation 3)}$$

In our model, there are four different promotor states: LTR is the free state, LTR* is the activated state but without RNAP binding; LTR-P and LTR*-P are the corresponding RNAP-bounded states. AC is assumed to promote LTR transiting to the activated state LTR*, e.g. LTR bound with NF-κ B, and LTR* recruits RNA polymerase much easier than LTR itself, e.g. the NF-κ B bound to LTR acting as a Transcription Factor to recruit RNA polymerase to LTR (Barboric et al., 2001). It has been shown that the screened Noise Enhancer has no effect on post transcription Dar et al. (2014), and some NE can increase transcription factors in cells, such as SP1 (Asin et al., 2008; Katagiri et al., 2006). Similar to (Dar et al., 2014), we assume that NE, once present, can slows down the switching rates between LTR and LTR-P.

We used Markov jumping process to model the transition among LTR states with AC and/or NE added (Figure 3A). The four states can mutually transit. We assume $S = \{LTR, LTR^*, LTRP, LTR^*P\}$, use R represents

LTR state, R^* represents *LTR** state, R^*P represents *LTR*P* state, P represents *LTRP* state. Then $S = \{R, R^*, P, R^*P\}$. We denote that $ON = \{P, R^*P\}$, $OFF = \{R, R^*\}$. The generator matrix (transition rate matrix) is:

$$Q = \begin{bmatrix} k_R & k_{R,R^*} & k_{R,RP} & 0 \\ k_{R^*R} & k_{R^*} & 0 & k_{R^*,R^*P} \\ k_{P,R} & 0 & k_P & k_{P,R^*P} \\ 0 & k_{R^*P,R^*} & k_{R^*P,R^*} & k_{R^*P} \end{bmatrix} \qquad \text{(Equation 4)}$$

$$k_i = -\sum_j k_{i,j} \quad i,j \in S$$

Then we can calculate invariant distribution π:

$$\begin{bmatrix} \pi_R \\ \pi_{R^*} \\ \pi_P \\ \pi_{R^*P} \end{bmatrix}^T \begin{bmatrix} k_R & k_{R,R^*} & k_{R,P} & 0 \\ k_{R^*,R} & k_{R^*} & 0 & k_{R^*,R^*P} \\ k_{P,R} & 0 & k_P & k_{P,R^*P} \\ 0 & k_{R^*P,R^*} & k_{R^*P,P} & k_{R*P} \end{bmatrix} = \begin{bmatrix} 0 \\ 0 \\ 0 \\ 0 \end{bmatrix}^T \qquad \text{(Equation 5)}$$

More specifically, here we assume in the absence of AC, RNAP binds to LTR at a relatively slow rate $k_{bindp}[P]$ and unbinds fast at rate $k_{unbindp}$; LTR transit to LTR* state with an extremely slow rate k_{act} without AC, but at a much higher rate $k_{act}\gamma$ ($\gamma \gg 1$) once AC is present; RNAP is attracted to bind to LTR* at a higher rate ωk_{bindp}, where ω is the cooperative interaction factor ($\omega > 1$); when NE is added, LTR will bind and unbind RNAP at a slower rate ($k_{bindp}e^{-\alpha}$, $k_{unbindp}e^{-\alpha}$) with a reduction parameter $\alpha = 0$; LTR-P and LTR*-P can mutually transit at rate $\omega k_{act}\gamma$ and rate k_{unact}.

Here, there is no external energy input; it is under detailed balance condition:

$$k_{R,R^*}k_{R^*,R^*P}k_{R^*P,P}k_{P,R} = k_{R,P}k_{P,R^*P}k_{R^*P,R^*}k_{R^*,R}$$

where $k_{R,R^*} = k_{act}\gamma$, $k_{R^*,R^*P} = \omega k_{bindp}$, $k_{R^*P,P} = k_{unact}$, $k_{P,R} = k_{unbindp}e^{-\alpha}$, $k_{R,P} = k_{bindp}e^{-\alpha}$, $k_{P,R^*P} = \omega k_{act}\gamma$, $k_{R^*P,R^*} = k_{unbindp}$, $k_{R^*,R} = k_{unact}$.

Non-Detailed-Balance LTR-4-state model

Breaking the detailed balance condition in the Detailed Balance LTR-4-state model, we can build non-Detailed-Balance LTR-4-state models. We first built it with energy input only through a single transition: Energy input can influence any single transition rate in the Detailed Balance LTR-4-state model through multiplying it by a factor of e^β. Such an energy input will cause clockwise (c.w.) probability flux or counter-clockwise (c.c.w.) probability flux. The details of the non-Detailed-Balance model are listed in Table S3.

We also built an EITST (Energy Input on the Two Specific Transition rates) LTR-4-state model, in which part of the energy input is through reducing the transition rate from LTR*-P to LTR* by multiplying $e^{-\beta_2}$, and the other part is through increasing the transition rate from LTR*-P to LTR-P by multiplying e^{β_1} (Figure 5A), instead of with total energy input on a single transition. The details of the EITST model are shown below.
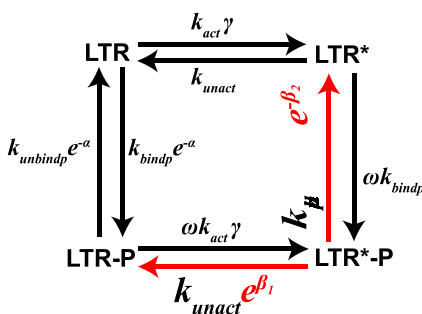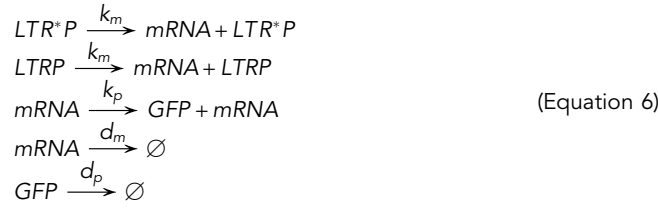

Figure. The rate formula in EITST model

GFP expression without feedback, calculation of mean and noise of LTR

We describe the dynamics of LTR-GFP vector expression using the following chemical reactions (combined with reactions Equation (3)):

$$LTR^*P \xrightarrow{k_m} mRNA + LTR^*P$$
$$LTRP \xrightarrow{k_m} mRNA + LTRP$$
$$mRNA \xrightarrow{k_p} GFP + mRNA \qquad \text{(Equation 6)}$$
$$mRNA \xrightarrow{d_m} \varnothing$$
$$GFP \xrightarrow{d_p} \varnothing$$

For the LTR-GFP vector, with RNAP bond to LTR (i.e. LTR-P state or LTR*-P state), the downstream DNA of LTR can be transcribed into mRNA at rate k_m and then translate into protein at rate k_{GFP}. Also, mRNA and GFP will degrade at rate d_m and d_{GFP} respectively (Figure 3B). To Calculate the Noise and Mean of GFP of this system, we need calculate the first and second moment of GFP:

$$\langle GFP \rangle(t) = \sum_{i \in S} \sum_{m=0}^{\infty} \sum_{n=0}^{\infty} n P(LTR = i, mRNA = m, GFP = n, t)$$

and

$$\langle GFP^2 \rangle(t) = \sum_{i \in S} \sum_{m=0}^{\infty} \sum_{n=0}^{\infty} n^2 P(LTR = i, mRNA = m, GFP = n, t)$$

Here, $P(LTR = i, mRNA = m, t)$ represents the probability of LTR staying at i state and $\#mRNA = m$ at time m; $P(LTR = i, mRNA = m, GFP = n)$ represents the probability of LTR staying at i state and $\#mRNA = m$ and $\#GFP = n$ at time t. For the following, when the variable/quantity/moment is not written as an explicit function of time t, it mean the steady state value. Then we sum up the related master equation and calculate the steady state (the derivative is zero):

$$\langle GFP \rangle = \frac{k_p}{d_p} \langle mRNA \rangle \qquad \text{(Equation 7)}$$

and

$$\langle GFP^2 \rangle = \frac{k_p}{d_p} (\langle GFP \; mRNA \rangle + \langle mRNA \rangle) \qquad \text{(Equation 8)}$$

To calculate the above quantity, we need calculate the following moments of mRNA and GFP:

$$\langle mRNA \rangle(t) = \sum_{i \in S} \sum_{m=0}^{\infty} m P(LTR = i, mRNA = m, t)$$

$$\langle mRNA^2 \rangle(t) = \sum_{i \in S} \sum_{m=0}^{\infty} m^2 P(LTR = i, mRNA = m, t)$$

$$\langle GFP \; mRNA \rangle(t) = \sum_{i \in S} \sum_{m=0}^{\infty} \sum_{n=0}^{\infty} mn P(LTR = i, mRNA = m, GFP = n, t)$$

and similarly, we sum up the related master equation and calculate the steady state (the derivative is zero), followed by

$$\langle mRNA \rangle = \frac{1}{d_m} \sum_{i \in S} k_{m,i} \pi_i \qquad \text{(Equation 9)}$$

$$\langle GFP \; mRNA \rangle = \frac{\sum_{i \in S} k_{m,i} \langle GFP \rangle_i + k_p \langle mRNA^2 \rangle}{d_m + d_p} \qquad \text{(Equation 10)}$$

$$\langle mRNA^2 \rangle = \frac{1}{d_m} \sum_{i \in S} k_{m,i} \langle mRNA \rangle_i + \frac{1}{d_m} \sum_{i \in S} k_{m,i} \pi_i \qquad \text{(Equation 11)}$$

where

$$k_{m,i} = \begin{cases} k_m, i \in ON \\ 0, i \in OFF \end{cases}$$

$$\langle mRNA \rangle_i = \sum_{m=0}^{\infty} m P(LTR = i, mRNA = m)$$

$$\langle GFP \rangle_i = \sum_{n=0}^{\infty} n \sum_{m=0}^{\infty} P(LTR = i, mRNA = m, GFP = n)$$

for all $i \in S$. $\langle mRNA \rangle_i$ and $\langle GFP \rangle_i$ satisfy the linear equations (the steady state of Master Equations):

$$(d_m I_4 - Q) \begin{bmatrix} \langle mRNA \rangle_R \\ \langle mRNA \rangle_{R^*} \\ \langle mRNA \rangle_P \\ \langle mRNA \rangle_{R^*P} \end{bmatrix} = \begin{bmatrix} k_{m,R}\pi_R \\ k_{m,R^*}\pi_{R^*} \\ k_{m,P}\pi_P \\ k_{m,R^*P}\pi_{R^*P} \end{bmatrix} \qquad \text{(Equation 12)}$$
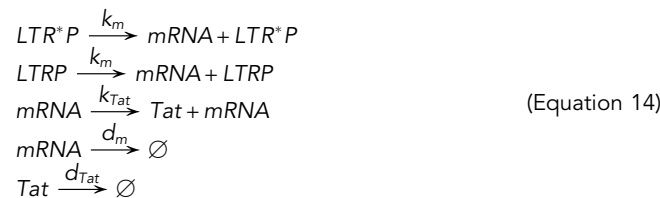
$$(d_p I_4 - Q) \begin{bmatrix} \langle GFP \rangle_R \\ \langle GFP \rangle_{R^*} \\ \langle GFP \rangle_P \\ \langle GFP \rangle_{R^*P} \end{bmatrix} = k_P \begin{bmatrix} \langle mRNA \rangle_R \\ \langle mRNA \rangle_{R^*} \\ \langle mRNA \rangle_P \\ \langle mRNA \rangle_{R^*P} \end{bmatrix} \qquad \text{(Equation 13)}$$

where I_4 is the 4×4 identity matrix, Q is the generator matrix for the LTR-4-state model.

We solved the linear equations Equations (12), (13), then substituted $\langle mRNA \rangle_i$ and $\langle GFP \rangle_i$ for $i \in S$ into equations Equations (10), (11). We then substituted Equations (9), (10), (11) into equations Equations (7), (8). Using the above calculation and submission, we have the Noise of LTR-GFP vector, $\frac{\langle GFP^2 \rangle - \langle GFP \rangle^2}{\langle GFP \rangle^2}$, and the mean of LTR-GFP vector, $\langle GFP \rangle$.

Tat expression with positive feedback

We describe the dynamics of the full length HIV vector expression with Tat positive feedback using the following chemical reactions (combined with reactions Equation (3)):

$$
\begin{aligned}
LTR^*P &\xrightarrow{k_m} mRNA + LTR^*P \\
LTRP &\xrightarrow{k_m} mRNA + LTRP \\
mRNA &\xrightarrow{k_{Tat}} Tat + mRNA \\
mRNA &\xrightarrow{d_m} \varnothing \\
Tat &\xrightarrow{d_{Tat}} \varnothing
\end{aligned}
\qquad \text{(Equation 14)}
$$

The Tat forms positive feedback by enhancing the elongation of initial transcribed mRNA of HIV (Feinberg et al., 1991; Frankel, 1992) and by stabilizing the HIV activation (Razooky et al., 2015). We model these two functions by following:

$$k_m = k_{mbasal} + k_{trs1}\frac{\frac{Tat}{k_{trs2}}}{1 + \frac{Tat}{k_{trs2}}} \qquad \text{(Equation 15)}$$

and

$$k_{unbindp} = \frac{k_{threshold}^3 + \delta Tat^3}{k_{threshold}^3 + Tat^3}k_{unbindp0} \qquad \text{(Equation 16)}$$

All parameter values are shown in Table S4.

To prove the model results does not depend on Tat active degradation, we also performed the simulation with cell division. Similar as previous works simulating cell division (Zhao et al., 2021), in our corresponding SSA, every time the updated time passes one cell cycle length, the system will execute cell division, where Tat concentration will be diluted to half of its concentration. The simulation results shown in Figure S12.

Using Tat-binding states to model Tat positive feedback to prove the results is independent from the specific details of the model, we also applied another model adapted from (Razooky et al., 2015) shown below.
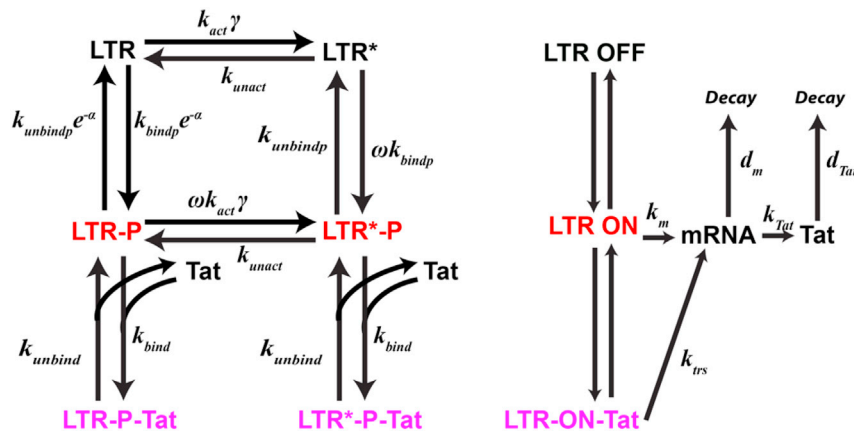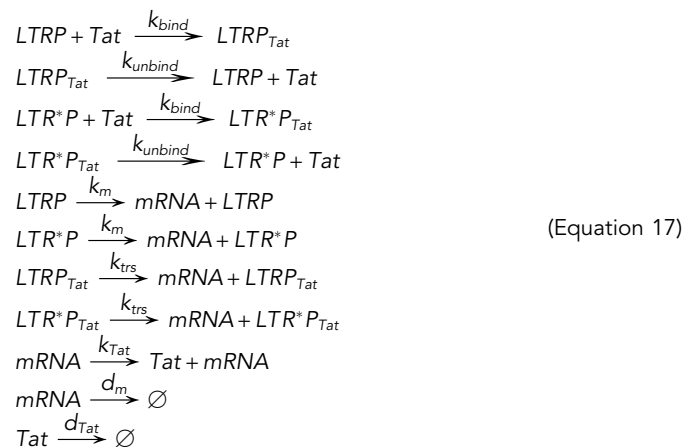
Figure. The scheme of LTR-six-state model

In this model, similar to LTR-2-state Tat positive feedback model, the Tat forms positive feedback through binding to LTR(TAR) Tat can bind/unbind to LTR(TAR) with rate k_{bind} and k_{unbind}, then transactivate LTR-on state once bound to TAR with a much higher transcription rate k_{trs} than the transcription rate k_m at LTR-on state due to Tat's enhancing LTR transcriptional elongation. The system can be expressed by the following chemical reactions (combined with reactions Equation (3)):

$$
\begin{aligned}
LTRP + Tat &\xrightarrow{k_{bind}} LTRP_{Tat} \\
LTRP_{Tat} &\xrightarrow{k_{unbind}} LTRP + Tat \\
LTR^*P + Tat &\xrightarrow{k_{bind}} LTR^*P_{Tat} \\
LTR^*P_{Tat} &\xrightarrow{k_{unbind}} LTR^*P + Tat \\
LTRP &\xrightarrow{k_m} mRNA + LTRP \\
LTR^*P &\xrightarrow{k_m} mRNA + LTR^*P \\
LTRP_{Tat} &\xrightarrow{k_{trs}} mRNA + LTRP_{Tat} \\
LTR^*P_{Tat} &\xrightarrow{k_{trs}} mRNA + LTR^*P_{Tat} \\
mRNA &\xrightarrow{k_{Tat}} Tat + mRNA \\
mRNA &\xrightarrow{d_m} \varnothing \\
Tat &\xrightarrow{d_{Tat}} \varnothing
\end{aligned}
$$

(Equation 17)

All parameter values are the same as LTR-2-state Tat positive feedback model, shown in Table S1.

QUANTIFICATION AND STATISTICAL ANALYSIS

Mathematical analysis of LTR-4-state model

Probability of LTR-on states P_{on}

From Equation (5), we have invariant distribution of LTR-4-state model, π_i for $i \in S$. We then calculated the probability of LTR-on states (LTR-P state and LTR*-P state):

$$P_{on} = \pi_P + \pi_{R^*P}$$

Probability flux and cycle flux

From invariant distribution Equation (5) and the transition rates, we can calculate the probability flux of LTR-4-state model at steady state:

$$j_{ij} = \pi_i k_{i,j}$$

for $i,j \in S$. And net flux from state I to state j is defined as $J_{ij} - J_{ji}$. In such a 4-state model, there is only one cycle (LTR- > LTR*- > LTR*-P- > LTR-P- > LTR), which is clockwise, and its reversed one. The net cycle flux of the clockwise cycle is $J_c = J_{R,R*} = J_{R*,R*P} = J_{R*P,RP} = J_{RP,R}$, and the net flux of the reversed counterclockwise cycle is $-J_c$.

Reactivation ratio

The stochastic LTR-4-state model coupled with Tat positive feedback (Equations (3), (14), (15), and (16)) was simulated using the Stochastic Simulation Algorithm (SSA), or say 'Gillespie' algorithm (Gillespie, 1977), because of the difficulty to analytically calculate the model with feedback.

The reactivation ratio is the ratio of activated HIV (#Tat >75), where the trajectory number is 100 h and the total number of trajectories starts from the latent state (LTR = 1, copy numbers of all other species = 0, simulated 5000~10000 cells) at time 0h. These simulations were implemented via MATLAB™ with the parameters shown in Tables S3 and S4.

Mean duration time

We need a theorem to calculate mean duration time.

Theorem (Jia et al., 2009)

Let $\{X_t, t \geq 0\}$ be a continuous time Markov chain on state space S, with generator matrix $Q = (q_{ij})$. S_1 and S_2 are subspaces of S satisfying:

$$S = S_1 \cup S_2, S_1 \cap S_2 = \varnothing, S_1 \neq \varnothing, S_2 \neq \varnothing$$

Suppose the invariant distribution $\mu = \{\mu : \iota \in S\}$ exists, then the mean duration in S_1 (denoted by τ) takes the form of

$$\tau = \frac{\sum_{i \in s_1} \mu_i}{\sum_{i \in s_1} \sum_{j \in s_1} \mu_i q_{ij}}$$

See (Jia et al., 2009) for proof.

For the LTR-4-state continuous time Markov chain with transitions showed in Equations Equation (3), the generator Q is Equation (4), and the invariant distribution π_i for $i \in S$ can be derived from linear Equations Equation (5). We assume that $S_1 = ON = \{LTRP, LTR^*P\}$, $S_2 = OFF = \{LTR, LTR^*\}$. We define $\tau_{ON}(\tau_{OFF})$ as the mean duration time of LTR stay at ON(OFF) states. By the theorem, we have:

$$\tau_{ON} = \frac{\sum_{i \in ON} \pi_i}{\sum_{i \in ON} \sum_{j \in OFF} \pi_i q_{ij}}$$

$$\tau_{OFF} = \frac{\sum_{i \in OFF} \pi_i}{\sum_{i \in OFF} \sum_{j \in ON} \pi_i q_{ij}}$$

f_{inh}, the degree of AC's inhibition upon the reduction of λ_{on} induced by NE

We regarded the reciprocal of the Mean Duration Time as the transition rates between LTR-on and LTR-off states, λ_{on} and λ_{off},

$$\begin{cases} \lambda_{on} = \dfrac{1}{\tau_{OFF}} \\ \\ \lambda_{off} = \dfrac{1}{\tau_{ON}} \end{cases}$$ (Equation 18)

which are equivalent to k_{on} and k_{off} in the effective LTR-2-State model. Then we defined the effective f_{inh} using the formula Equation (2), i.e.

$$f_{inh} = \frac{1n(\lambda_{on,AC,NE}) - 1n(\lambda_{on,AC})}{1n(\lambda_{off,AC}) - 1n(\lambda_{off,AC,NE})} + 1$$ (Equation 19)

$\lambda_{on,AC}$ and $\lambda_{off,AC}$ correspond to the LTR-state model with only AC added, i.e. $\gamma \gg 1$, $\alpha = 0$; $\lambda_{on,AC,NE}$ and $\lambda_{off,AC,NE}$ correspond to the LTR-state model with both AC and NE added, i.e. $\gamma \gg 1$, $\alpha > 0$. Similar we can define $\lambda_{on,AC,NS}$ and $\lambda_{off,AC,NS}$.

Theorem on the relation between drug synergy of P_{on} and cyclic probability flux

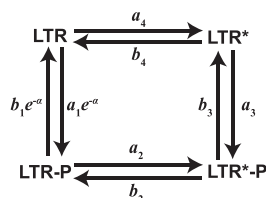Generally, our non-detailed-balanced LTR-4-state model can be described as below:

Figure. The scheme of LTR-four-state model and the symbols used in the proof

The corresponding Chemical Master Equations are

$$\begin{cases} \dfrac{d\,P_{LTR}}{d_t} = -\,(a_1 e^{-\alpha} + a_4)P_{LTR} + b_1 e^{-\alpha} P_{LTRP} + b_4 P_{LTR^*} \\[2mm] \dfrac{d\,P_{LTRP}}{dt} = a_1 e^{-\alpha} P_{LTR} - (b_1 e^{-\alpha} + a_2)P_{LTRP} + b_2 P_{LTR^*P} \\[2mm] \dfrac{d\,P_{LTR^*P}}{dt} = a_2 P_{LTRP} - (b_2 + b_3)P_{LTR^*P} + a_3 P_{LTR^*} \\[2mm] \dfrac{d\,P_{LTR^*}}{dt} = a_4 P_{LTR} + b_3 P_{LTR^*P} - (b_4 + a_3)P_{LTR^*} \end{cases}$$

At steady state, the derivative is zero. Then, with the net flux J introduced, the equations above at steady state can be simplified to a set of equations:

$$\begin{cases} J = -\,a_1 e^{-\alpha} P_{LTR} + b_1 e^{-\alpha} P_{LTRP} \\ J = -\,a_2 P_{LTRP} + b_2 P_{LTR^*P} \\ J = -\,b_3 P_{LTR^*P} + a_3 P_{LTR^*} \\ J = -\,b_4 P_{LTR^*} + a_4 P_{LTR} \end{cases} \qquad \text{(Equation 20)}$$

Here, $J > 0$ indicates a clockwise cycle net flux while $J < 0$ means a counter-clockwise one. And note that **synergy** of P_{on} is defined as the increase of $P_{on}(\alpha) = P_{LTRP}(\alpha) + P_{LTR^*P}(\alpha)$ when there exists NE ($\alpha > 0$) and the decrease of $P_{on}(\alpha)$ when NS is present ($\alpha < 0$), compared with P_{on} in the merely-AC case. ($\alpha = 0$)

Theorem 1

For any positive α_i and $b_i(i = 1, 2, 3, 4)$,

(1) If $J > 0$, then $P_{on}(\alpha) > P_{on}(0)$ for $\alpha > 0$ and $P_{on}(\alpha) < P_{on}(0)$ for $\alpha < 0$;

(2) If $J < 0$, then $P_{on}(\alpha) < P_{on}(0)$ for $\alpha > 0$ and $P_{on}(\alpha) > P_{on}(0)$ for $\alpha < 0$.

Proof

We begin with the case of $\alpha = 0$. From the kinetics equations Equation (20), we can eliminate the probabilities at the OFF state:

$$P_{LTR} = -\frac{J}{a_1} + \frac{b_1}{a_1}P_{LTRP},$$

$$P_{LTR^*} = -\frac{a_1 + a_4}{a_1 b_4}J + \frac{a_4 b_1}{a_1 b_4}P_{LTR}.$$

Therefore,

$$\left(1 + \frac{a_3(a_1 + a_4)}{a_1 b_4}\right)J = -b_3 P_{LTR^*P} + \frac{a_3 a_4 b_1}{a_1 b_4} P_{LTRP},$$
$$J = b_2 P_{LTR^*P} - a_2 P_{LTRP},$$

and

$$P_{LTRP} = \frac{a_1 b_4 (b_2 + b_3) + a_3 b_2 (a_1 + a_4)}{a_3 a_4 b_1 b_2 - a_1 a_2 b_3 b_4} J,$$
$$P_{LTR^*P} = \frac{a_1 a_2 (a_3 + b_4) + a_3 a_4 (a_2 + b_1)}{a_3 a_4 b_1 b_2 - a_1 a_2 b_3 b_4} J.$$

Since $P_{LTR} + P_{LTR^*} + P_{LTRP} + P_{LTR^*P} = 1$ gives that

$$-\frac{J}{a_1} + \frac{b_1}{a_1} P_{LTRP} - \frac{a_1 + a_4}{a_1 b_4} J + \frac{a_4 b_1}{a_1 b_4} P_{LTRP} + P_{LTRP} + P_{LTR^*P} = 1,$$

we have

$$-\frac{a_1 + a_4 + b_4}{a_1 b_4} + \frac{a_4 b_1 + b_1 b_4 + a_1 b_4}{a_1 b_4} \frac{a_1 b_4 (b_2 + b_3) + a_3 b_2 (a_1 + a_4)}{a_3 a_4 b_1 b_2 - a_1 a_2 b_3 b_4} + \frac{a_1 a_2 (a_3 + b_4) + a_3 a_4 (a_2 + b_1)}{a_3 a_4 b_1 b_2 - a_1 a_2 b_3 b_4} = \frac{1}{J}.$$

By replacing a_1 and b_1 with $a_1 e^{-\alpha}$ and $b_1 e^{-\alpha}$, we obtain the general equality:

$$a_1(a_2 a_3 + a_2 b_3 + a_2 b_4 + a_3 b_2 + b_2 b_4 + b_3 b_4) + e^{\alpha}(a_2 a_3 a_4 + a_2 a_4 b_3 + a_2 b_3 b_4 + a_3 a_4 b_2)$$
$$+ b_1(a_3 a_4 + a_3 b_2 + a_4 b_2 + a_4 b_3 + b_2 b_4 + b_3 b_4) = \frac{a_3 a_4 b_1 b_2 - a_1 a_2 b_3 b_4}{J(\alpha)}.$$

It is easy to see that:

(1) $J(\alpha)$ decreases with α when $J > 0$ and increases with α when $J < 0$, i.e.

$$\begin{aligned} J(0) - J(\alpha) > 0, \quad \text{if } J > 0 \\ J(0) - J(\alpha) < 0, \quad \text{if } J < 0 \end{aligned} \qquad \text{(Equation 21)}$$

(2) $e^{\alpha} J(\alpha)$ increases with α when $J > 0$ and decreases with α when $J < 0$;

$$\begin{aligned} e^{\alpha} J(\alpha) - J(0) > 0, \quad \text{if } J > 0 \\ e^{\alpha} J(\alpha) - J(0) < 0, \quad \text{if } J < 0 \end{aligned} \qquad \text{(Equation 22)}$$

(3) $J(\alpha)$ shares the same sign with $J(0)$.

$$J(\alpha) J(0) > 0$$

When NE/NS concentration approaches zero which means $\alpha = 0$, our model reduces to the general equality in Jia et al. (2012):

$$P_{on}(\alpha) - P_{on}^0 = \left(P_{on}^{\infty} - P_{on}^0\right) P_{on}(\alpha) - \left(\frac{P_{on}^{\infty}}{a_3} - \frac{P_{on}^0}{a_1}\right) J, \qquad \text{(Equation 23)}$$

where $P_{on}^0 = \frac{a_1}{a_1 + b_1}$, $P_{on}^{\infty} = \frac{a_3}{a_3 + b_3}$ remain the same under any value of α. From Equation (23), we have:

$$\left(1 - P_{on}^{\infty} + P_{on}^0\right) P_{on}(\alpha) = P_{on}^0 - \left(\frac{P_{on}^{\infty}}{a_3} - \frac{P_{on}^0}{a_1}\right) J, \qquad \text{(Equation 24)}$$

To calculate the synergy $P_{on}(\alpha) - P_{on}(0)$, we subtract equation Equation (24) with $\alpha = 0$ from equation Equation (24) with $\alpha > 0$ (NE), and we have:

$$\left(1 - P_{on}^{\infty} + P_{on}^{\infty}\right)\left(P_{on}(\alpha) - P_{on}(0)\right) = -\left(\frac{1}{a_3 + b_3} - \frac{e^{\alpha}}{a_1 + b_1}\right)J(\alpha) + \left(\frac{1}{a_3 + b_3} - \frac{1}{a_1 b_1}\right)J(0)$$

$$= \frac{J(0) - J(\alpha)}{a_3 + b_3} + \frac{e^{\alpha}J(\alpha) - J(0)}{a_1 + b_1}.$$

(Equation 25)

Since $1 - P_{on}^{\infty} + P_{on}^{0} > 0$, and for clockwise cyclic probability flux ($J > 0$), substitute Equations (21), (22) into (25), we can prove that such case predicts positive synergy.

Similarly, for clockwise cyclic probability flux ($J > 0$), for the effect of NS ($\alpha < 0$),

$$\left(1 - P_{on}^{\infty} + P_{on}^{0}\right)\left(P_{on}(\alpha) - P_{on}(0)\right) = \frac{J(0) - J(\alpha)}{a_3 + b_3} + \frac{e^{\alpha}J(\alpha) - J(0)}{a_1 + b_1} < 0$$

which shows that the LTR-4-state model with clockwise cyclic probability flux distinguishes NE and NS well.

Since the monotonicity of both $J(\alpha)$ and $e^{\alpha}J(\alpha)$ gets reverse, by the same token we can prove that for counter-clockwise cyclic probability flux ($J < 0$), $P_{on}(\alpha) - P_{on}(0) < 0$ and no synergy is predicted when $\alpha > 0$ (NE), while $P_{on}(\alpha) - P_{on}(0) > 0$ when $\alpha > 0$ (NS).

Distribution of duration time at LTR-on/off states in equilibrium system

According to Tu (2008), the distribution of duration time at LTR-on/off states in equilibrium system should be monotonically decreasing and convex, while in the nonequilibrium system these features can be violated. We use the following equations to calculate the distribution of duration time at LTR-off states:

$$\frac{dQ(LTR, \tau)}{d\tau} = k_{R^*,R} Q(LTR^*, \tau) - k_{R,P} Q(LTR, \tau)$$

$$\frac{dQ(LTR^*, \tau)}{d\tau} = -k_{R^*,R} Q(LTR^*, \tau) + k_{R,R^*} Q(LTR, \tau) - k_{R^*,R^*P} Q(LTR^*, \tau)$$

With initial conditions:

$$Q(LTR, 0) = A_{off} k_{P,R} \pi_P$$
$$Q(LTR^*, 0) = A_{off} k_{R^*P,R^*} \pi_{R^*P}$$

Where

$$A_{off} = \frac{1}{k_{P,R} \pi_P + k_{R^*P,R^*} \pi_{R^*P}}$$

The distribution of duration time at LTR-off states can be expressed:

$$P_{off}(\tau) = k_{R,P} Q(LTR, \tau) + k_{R^*,R^*P} Q(LTR^*, \tau)$$